東北大学機関リポジトリ
TOUR
Tohoku University Repository
東北大学

Association of Similarity between Maternal and Fetal RR Interval with Fetal Development in Humans and Mice

著者	Widatalla Namareq Salah Mohamed
学位授与機関	Tohoku University
URL	http://hdl.handle.net/10097/00137414

TOHOKU
UNIVERSITY

博 士 学 位 論 文

論文題目 Association of Similarity between Maternal and Fetal RR Interval with Fetal Development in Humans and Mice

ヒトおよび゛マウスにおける母と胎児の RR 間隔の類似性と胎児発達との関係

提 出 者　**東北大学大学院医工学研究科**

医工学専攻

学籍番号　C0WD1008

氏　　名　Namareq Salah Mohamed Widatalla

指導教員	齋藤　昌利　　(教授)・准教授	
審査委員 （○印は主査）	○　齋藤　昌利　教授	
	1　永富　良一　教授	2　西條　芳文　教授
	3　船本　健一　准教授	4
	5	6

提出者略歴	
ふりがな 氏名　なまれっく　さら　もはまど　うぃだたら Namareq Salah Mohamed Widatalla	昭和 (平成) 西暦　3年　7月　25日生
本籍　都・道 府・県	国籍　スーダン

履歴事項	
【学　歴】	
平成 21 年　9 月　日	Enrolled as an undergraduate student at Khalifa University, UAE
平成 26 年　3 月　日	Obtained the Bachelor degree from the biomedical department, Khalifa University, UAE
平成 30 年　4 月　1 日	Enrolled in the Master's program at the Graduate School of Biomedical Engineering, Tohoku University, Japan
令和　2 年　3 月　25 日	Completed the Master's program at the Graduate School of Biomedical Engineering, Tohoku University, Japan
令和　2 年　4 月　1 日	Enrolled in the PhD program at the Graduate School of Biomedical Engineering, Tohoku University, Japan
令和　5 年　3 月　24 日	Completed the PhD program at the Graduate School of Biomedical Engineering, Tohoku University, Japan
【職　歴】	
平成 27 年　8 月　1 日	Khalifa University, UAE 入職
平成 27 年　12 月　31 日	Khalifa University, UAE 退職
平成 28 年　10 月　1 日	Khalifa University, UAE 入職
平成 29 年　3 月　31 日	Khalifa University, UAE 退職

備考 1）外国人留学生は、国籍を記入してください。

2）履歴事項は、大学入学から年次にしたがって記入してください

Abstract

Maternal behavior during the prenatal period was associated with the offspring's well-being and, according to the fetal programming theory, maternal influence during the same period may extend to adulthood. Over the past decades, many studies investigated the maternal impact on fetal health. For example, previous studies investigated the effect of maternal weight and age on fetal well-being and birth outcomes. During the prenatal period, fetal health is largely monitored by fetal heart rate (fHR) measurements, hence, various research tried to understand the maternal influence on fetal development by studying the correlation between maternal and fetal HR. Previously, correlations between maternal and fetal HR were investigated by assessing the correlation between their average HR collected over a period of time, and by beat-by-beat coupling analysis. However, so far, there is a lack of knowledge regarding how maternal-fetal HR interaction or coupling is associated with fetal development.

In this thesis, the existence of similarity between maternal and fetal RR interval (RRI) is discussed. To our knowledge, the presence of the same similarity has not been discussed in previous literature. The degree of similarity was assessed by conducting a cross-correlation (CC) analysis between maternal and fetal RRI tachograms. Correlation analysis between the CC coefficients and fetal age revealed that similarity between maternal and fetal RRI is associated with fetal development. The previous analysis was conducted by using RRI signals that were calculated from electrocardiogram (ECG) records. The ECG records were collected from human and mouse subjects.

To explore further, the association of maternal and fetal HR variability (HRV) with the CC coefficients was investigated and the results showed that the similarity is associated with the maternal very low frequency (mVLF). Because fetal RRI (fRRI) was found to be similar to that of the mother, correlation analysis between maternal and fetal HRV was performed in this study. The result of correlation analysis showed that positive correlations exist between maternal and fetal HRV. Also, an artificial intelligence (AI) based model was developed to predict fRRI from maternal factors that included age, weight, and ECG-derived features.

In addition to the above, the similarity patterns in the spectrum autism disorder (ASD) mouse model were investigated and compared with that of typical development. The comparison showed that the CC coefficients were lower in ASD mouse model suggesting that disturbances in maternal-fetal RRI similarity are a feature of ASD during the prenatal period. The findings entailed in this thesis emphasize the importance of maternal health on fetal development and well-being. Also, it highlights the potential of assessing maternal-fetal RRI similarity patterns to monitor fetal development.

Acknowledgments

My deepest appreciation goes to my supervisors Prof. Masatoshi Saito, Prof. Yoshitaka Kimura, and Dr. Yoshiyuki Kasahara for their massive support and guidance. In addition, special thanks go to Prof Ryoichi Nagatomi for his valuable advice that assisted me during my research. I would like to thank the thesis committee: Prof. Yoshifumi Saijo, Prof. Ryoichi Nagatomi, and Prof. Kenichi Funamoto for their valuable comments and feedback. I would like to express my gratitude to Chihiro Yoshida who has been a great support in writing up research papers and addressing reviews' feedback and comments. I would like to thank Kunihiro Koide who provided me with the necessary data to perform the research. Special thanks go to the rest of the laboratory team members.

In addition to the academic support, I would like to express my gratitude to all members of the laboratory. Living in a foreign country has its challenges but because of the support I received from all members, I was able to continue my studies. On a special note, I am grateful for the enormous amount of support that I received from Chie Yoshida. She was a great help when I needed consultations and advice regarding different matters. Also, she has been a great help in my Japanese language studies. I would like to thank also Dr. Kiyoe Funamoto who has been a great source of encouragement to me and assisted me in different aspects that included daily life and academics.

From Khalifa University, I would like to thank Prof. Ahsan Khandoker and Mohanad Alkhodari who provided me with guidance and great advice that enabled be achieve my milestones.

My deepest thanks go to my parents (Salah & Suad) and siblings (Tasneem, Mohamed, Alaa & Ahmed) who have been always by my side during the good and bad times. Also, my deepest thanks extend to my friends in Japan, UAE, USA, and Canada who have been always supporting me.

Content

Abstract ... iii
Acknowledgments ... iv
List of Figures ... viii
List of Tables ... xi
Abbreviations ... xii
Chapter 1: Introduction ... 1
1.1 Background and motivation ... 1
1.2 Contribution ... 2
1.3 Aims ... 2
1.4 Thesis outline ... 2
1.5 Research publications ... 3
Chapter 2: Literature Review ... 4
2.1 Brief review of maternal-fetal HR relations ... 4
2.2 Brief review of the relationship between maternal condition and fetal HR or HRV ... 10
2.3 Conclusion ... 12
Chapter 3: Maternal-fetal RRI similarity ... 13
3.1 Brief overview of the chapter ... 13
3.2 Methods ... 15
3.2.1 Data Collection ... 15
3.2.2 Data selection and fetal ECG (fECG) extraction ... 15
3.2.3 Similarity quantification with CC analysis ... 16
3.2.4 Data classifications based on CC1 and CC3 ... 19
3.2.5 Statistical analysis ... 20
3.3 Demonstration of maternal-fetal RRI tachogram similarities ... 21
3.4 Similarities' association with fetal development ... 21
3.5 Similarities' association with HRV ... 23
3.6 Discussion and physiological implications ... 25
3.7 Limitations and Conclusion ... 28
Chapter 4: Pattern-based maternal-fetal HRV correlation ... 29
4.1 Brief overview of the chapter ... 29
4.2 Methods ... 31
4.2.1 Data selection and analysis ... 31
4.2.2 nRpp2s calculation ... 31

4.2.3 Statistical analysis 31
4.3 Demonstration of nRpp2s 31
4.4 Difference between maternal and fetal snRpp2s (dmf) 32
4.5 Correlation between maternal and fetal HRV per pattern 33
4.6 Discussion and physiological implications 34
4.7 Limitations and Conclusion 35
Chapter 5: Artificial intelligence-based model for fRRI prediction 36
5.1 Brief overview of the chapter 36
5.2 Methods 38
5.2.1 Data Selection 38
5.2.2 Heart rate variability (HRV) and R wave amplitude variability (RWAV) analysis 38
5.2.3 Machine learning models and Shapley analysis 38
5.2.4 Model evaluation 39
5.3 Results 40
5.3.1 Summary of the features 40
5.3.2 Comparison between SVR and RF performance 40
5.3.3 Shapley analysis 42
5.3.4 Model validation on test subjects 43
5.4 Discussion 43
5.5 Limitations and conclusion 44
Chapter 6: Maternal-fetal RRI similarities in mice 45
6.1 Brief overview of the chapter 45
6.2 Method 47
6.2.1 Animal handling 47
6.2.2 Experimental protocol 47
6.2.3 Data analysis 48
6.2.4 Measuring similarities between maternal and fetal RRI tachograms 49
6.2.5 Statistical analysis 49
6.3 Results 50
6.3.1 Fetal mouse development 50
6.3.2 ASD mouse model 53
6.4 Discussion and physiological implications 54
6.5 Use of mouse models to understand physiological processes 58
6.6 Conclusion and Limitation 59
Chapter 7: Conclusion 60
7.1 Conclusion and Future Work 60

Appendix A 62
Appendix B 63
Appendix C 64
Appendix D 65
Appendix E 66
Appendix F 70
References 71

List of Figures

Figure 1: Illustrative summary of chapter 3.....14

Figure 2: Example of a resampled signal. (A) Original maternal and fetal RR interval (RRI) tachograms. (B) Resampled RRI tachograms. Resampling was done by taking the average of RRI per 2 seconds. .18

Figure 3: Summary of data analysis. The flowchart provides a graphical summary of the steps that were followed to analyze the data. In Step 1, 5-minutes (mins) extraction of fetal electrocardiogram (fECG) was successful in 172 out of 195 subjects. In step 2, additional extraction of 5-min segments was successful in 158 out of the 172 subjects. Both in step 1 and step 2 cross-correlation (CC) and maternal and fetal heart rate variability (HRV) analyses were performed for the extracted 5-min segments. In step 3, a comparison of means analysis was performed to compare between group 1 and group 2 in terms of maternal and fetal HRV analysis. Group 2 has higher CC1 or CC3 values compared to group 1.....20

Figure 4: Demonstration of positive and negative similarity trends between maternal and fetal RR interval (RRI) tachograms. Figures A, B, and C (A-C) show examples of positive similarity trends in which maternal (blue) and fetal (orange) RRI tachograms change in the same direction. Figures D, E and F (D-F) show examples of negative similarity trends in which maternal and fetal RRI tachograms change in opposing directions. The upper panels in Figures D-F show the original signals while the lower panels show the original fetal signal with the maternal signal inversed. (A) The record belongs to a mother who had no records of medical complications, gestational age (GA): 20 weeks. (B) The record belongs to a mother with a record of uterine/appendix disease, GA: 23 weeks. (C) The record belongs to a mother with a medical record of respiratory disease and uterine/appendix disease, GA: 20 weeks. (D) The record belongs to a mother with a medical record of autoimmune disease, gestational age (GA): 39 weeks. (E) The record belongs to a mother who had a blood disease, GA: 33 weeks. (F) The record belongs to a mother with no records of medical complications, GA: 23 weeks. 22

Figure 5: Illustrative summary of chapter 4.....30

Figure 6: Demonstration of the number of R peaks per 2 seconds (nRpp2s): The upper panels show maternal (blue) and fetal (red) RR interval (RRI). The lower panels show the maternal and fetal number of R peaks per 2 seconds (nRpp2s). (A) The rate of change in mnRpp2s (blue) is higher than fnRpp2s (red), fetal standard deviation of nRpp2s (fsnRpp2s): 0.39, maternal snRpp2s (msnRpp2s): 0.51, GA: 37 weeks. The figure is an example of pattern 1. (B) The rate of change in maternal and fetal nRpp2s is roughly similar, fsnRpp2s: 0.35 msnRpp2s: 0.309, GA: 23 weeks, pattern 2. (C) Opposite to (A), the rate of change in fnRpp2s: 0.50 is higher than mnRpp2s: 0.37, GA: 29 weeks, pattern 3. 32

Figure 7: Demonstration of the maternal and fetal standard deviation of the number of R peaks per 2 seconds (snRpp2s) and their difference (dmf). (A) maternal (blue) and fetal (orange) snRpp2s show parabolic distribution with RR interval (RRI) and the difference between them (dmf) in (B) decreases

with gestational age (GA), r is the spearman correlation coefficient. The red dotted lines in (B) show the threshold values, - 0.05 and 0.05, that were used to divide the data into three patterns, pattern 1: dmf >= 0.05, pattern 2: 0.05 < dmf < - 0.05 and pattern 3: dmf <= - 0.05. The black dotted lines show the 95% confidence interval of regression between the dmf and GA..... 32

Figure 8: Illustrative summary of chapter 5..... 37

Figure 9: Summary of data analysis. Following extraction of maternal and fetal electrocardiogram (ECG), 13 features were calculated per 5-minute segments. The average from the two 5-minute segments was then fed to two models, support vector regression (SVR) and random forest (RF). 39

Figure 10: Absolute error percentage versus gestational age (GA). (A) support vector regression (SVR) model. (B) Random forest (RF) model. 41

Figure 11: Bland Altman (BA) and correlation analysis. (A) shows the results of the support vector machine (SVR) model and (B) shows the same for the random forest (RF) model. The limits of agreement of BA plot, root mean square error (RMSE), and error percentage are lower in the SVR model. Also, the spearman correlation coefficient (r) value of the SVR model is higher than that of the RF model. The latter facts show that the SVR model was more effective in the prediction of fRRI values. 41

Figure 12: Average Shapley values with 95% confidence interval (CI): Shapley analysis shows that age, HF, SDHR, and RRI had the highest impact on average fetal RR interval (fRRI) prediction whereas very high frequency (VHF) had the lowest impact. 42

Figure 13: Illustrative summary of Chapter 6. 46

Figure 14: Summary of electrocardiogram (ECG) analysis and similarity estimations. The figure provides (A) an illustrative summary of the protocols that were followed to analyze ECG data, (B) calculation of cross correlation (CC) coefficients and (C) coherence low frequency (CLF) and coherence high frequency (CHF) calculations. 50

Figure 15: Demonstration of maternal and fetal RR interval (RRI) similarities. All panels show resampled normalized maternal (blue) and fetal (red) RRI. (A) ED15.5, CCm1: 0.42, CCm2: 0.27, coherence low frequency (CLF): 0.084, coherence high frequency (CHF): 0.074. (B) ED18.5, CC1: 0.82, CC2: 0.67, CLF: 0.98, CHF: 0.92. (C) ED13.5, CCm1: 0.29, CCm2: - 0.18, CLF: 0.086, CHF: 0.074. (D) ED17.5, CCm1: 0.85, CCm2: - 0.85, CLF: 0.097, CHF: 0.088. 51

Figure 16: Example of similarity trend of two fetuses from the same mother. The figure shows resampled normalized maternal (blue) and fetal (red) RR interval (RRI) from embryonic day 17.5 (ED17.5). The top panel shows RRI for fetus 1 and the middle and bottom panels show the same for fetus 2. For fetus 1 (top panel), CCm1, CCm2, coherence low frequency (CLF) and coherence high

frequency (CHF) values were as follows, 0.92, 0.92, 0.098 and 0.093, respectively. For fetus 2, the same latter values were as follows: 0.83, - 0.60, 0.098 and 0.092, respectively. 52

Figure 17: Similarity coefficients at different developmental stages. The similarity between maternal and fetal RR interval (RRI) was quantified by using four coefficients: (A) CC1m(B) CCm2 (C) coherence low frequency (CLF). (D) coherence high frequency (CHF). The value of correlation between the coefficient and embryonic days (EDs) is indicated as r above the plot. 53

Figure 18: Comparison between saline (sal) group and valproic acid (VPA) groups at embryonic day (ED) 15.5 and ED18.5. (A) CCm1 coefficient. (B) CCm2 coefficient. (C) coherence low frequency (CLF) coefficient. (D) coherence high frequency (CHF) coefficient. 54

Figure 19: Comparison between saline and VPA in terms of fetal and maternal RRI correlation. (a) Maternal RRI is strongly positively correlated with fetal RRI in saline. (b) Maternal RRI is negatively correlated with fetal RRI in VPA. 57

Figure 20: Comparison between human and mouse fetal electrocardiogram (fECG) in terms of model-based estimation of an end of a T wave. This figure shows that a model-based estimation of end of a T wave occurs earlier in a mouse fECG compared to a human fECG. 58

List of Tables

Table 1: Summary of maternal and fetal HRV, CC coefficients and their correlations with GA, n=172. 23

Table 2: Comparison between group 1 and group 2 in terms of HRV and CC association with GA, n=158 24

Table 3: Comparison in means between Group 1 and Group 2 (n=158) 25

Table 4: Correlation between maternal and fetal HRV per pattern 33

Table 5: Mean and SD values of maternal features and fRRI 40

Table 6: SVR model prediction of fRRIs. 42

Table 7: Summary of sample size 48

Abbreviations

AI	Artificial Intelligence
ANS	Autonomic nervous system
ASD	Autism spectrum disorder
BA	Bland Altman
CC	Cross correlation
CHF	Coherence high frequency
CLF	Coherence low frequency
DOHaD	Developmental origins of health and diseases
ECG	Electrocardiogram
ED	Embryonic day
fECG	Fetal electrocardiogram
fHR	Fetal heart rate
fRRI	Fetal RR interval
fsnRRp2s	Fetal standard deviation of number of R peaks per 2 seconds
GA	Gestational age
HF	High frequency
HR	Heart rate
HRV	Heart rate variability
IUGR	Intrauterine growth restriction
LF	Low frequency
mECG	Maternal electrocardiogram
mRRI	Maternal RR interval
mVLF	Maternal very low frequency
msnRRp2s	Maternal standard deviation of number of R peaks per 2 seconds
MCG	Magnetocardiography
MSC	Magnitude-squared coherence
RWAV	R wave amplitude variability
RRI	RR interval

RF	Random Forest
RMSE	Root mean square error
snRpp2s	Standard deviation of number of R peaks per 2 seconds
SDHR	Standard deviation of heart rate
SDNN	Standard deviation of normal RR interval
SVM	Support vector machine
SVR	Support vector regression
dmf	Difference between maternal and fetal standard deviation of number of R peaks per 2 seconds
SD	Standard deviation
VHF	Very high frequency
VLF	Very low frequency

Chapter 1: Introduction

1.1 Background and motivation

The prenatal period features a unique bond between a mother and her child. During this period, the maternal body undergoes several changes to provide the optimal environment for child growth and birth (1). The fetus depends on the mother to survive, and lack of enough nourishment may affect fetal growth and birth outcomes. Maternal impact on fetal health was addressed previously by Barker, D (2) who mentioned that the maternal intrauterine environment can influence the offspring after birth. For example, it is believed that maternal-related factors, such as smoking and undernutrition, during the prenatal period could lead to intrauterine growth restriction (IUGR) or preterm birth (3). Based on Barker's theory, the idea of developmental origins of health and diseases (DOHaD) theory was developed. The theory states that some diseases may originate as early as the prenatal period (4).

The scope of investigating maternal influence on fetal health is huge as there are many factors to consider such as genetics, hormonal, physical, and many others. Previous literature attempted at understanding maternal influence on fetal healthy by using fetal heart rate (HR) and HR Variability (HRV) analysis and the reason for this can be summarized in two folds. First, a human fetus is inaccessible therefore, it is technically challenging to obtain blood samples directly from the fetus, especially before 18 weeks of gestation (5). Second, fetal HR and HRV are considered indicators of fetal growth and development (6,7), moreover, they can be measured non-invasively making them quick and efficient tools to assess fetal development. In addition to fetal HR and HRV, maternal HR and HRV were found to change during pregnancy and such changes are believed to occur to secure fetal growth and birth (8,9). Due to pregnancy, the mother is at risk of developing several complications such as preeclampsia (1,10). Therefore, simultaneous assessments of maternal and fetal HR can be used to monitor both maternal and fetal health.

Previously, it was reported that fetal HR (fHR) changed in harmony with maternal HR (mHR) throughout the day and such changes suggest the presence of interaction between both (11,12). In addition, the existence of beat-by-beat coupling and synchronization between both maternal and fetal HRs was reported (13,14,15), but the physiological implications behind them are not known yet. In

addition, their importance in assessing fetal development and maternal influences on fetal growth are yet to be explored.

1.2 Contribution

We have been working on developing methods to quantify maternal-fetal HR interaction to get insight into its association with fetal development and growth. Here, we focused our analysis on analyzing the simultaneous changes exhibited in maternal and fetal RR interval (RRI) tachograms. Visual inspection of maternal and fetal RRI tachograms revealed the presence of similarities between both, hence, we opted for quantifying the degree of association between them by means of CC analysis. Then, we investigated the association between similarities and fetal development in humans and mice. In addition, we investigated how the similarities may get disturbed in autism spectrum disorder (ASD) in mice.

1.3 Aims

The main aims of the thesis include:

- Highlight the presence of similarities between maternal and fetal RRI tachograms.
- Develop a method to quantify the similarities.
- Investigate the association of similarities with fetal development in mice and humans.
- Investigate how similarity patterns might get affected by ASD in mice.

1.4 Thesis outline

This thesis is divided into 6 main chapters excluding chapter 1. Chapter 2 provides a brief review of different literature that discussed maternal influence on fetal HR and HRV. In addition, examples of methods that were used previously to quantify maternal-fetal HR interaction are mentioned in chapter 2. Chapters 3, 4, and 5 discuss results from human subjects. In chapter 3, similarities between maternal and fetal RRI tachograms and their association with fetal development are discussed. Chapter 4 addresses correlations between maternal and fetal HRV. Chapter 5 entails artificial intelligence (AI) based prediction of fetal RRI (fRRI) from maternal factors. Chapter 6 discusses similarity patterns in typical development in mice, moreover, disturbance of the same patterns in the ASD mouse model is discussed. Chapter 7 concludes the thesis and addresses future directions of the work.

1.5 Research publications

Journal publications:

- Published

N. Widatalla, K. Funamoto, M. Kawataki, C. Yoshida, K. Funamoto, M. Saito, Y. Kasahara, A. Khandoker and Y. Kimura, "Model-based estimation of QT intervals of mouse fetal electrocardiogram," *Biomed. Eng. Online,* vol. 21, no. 45, 2022.

Widatalla N, Khandoker A, Alkhodari M, et al. Similarities between maternal and fetal RR interval tachograms and their association with fetal development. *Front. physiol*. Nov 2022.

Widatalla N, Khandoker A, Yoshida C, et al. Correlation between maternal and fetal heart rate increases with fetal mouse age in typical development and is disturbed in autism mouse model treated with valproic acid. *Front. Psychiatry.* Nov 2022.

- Under Review

Widatalla N, Alkhodari M, Koide K, et al. Prediction of fetal RR interval from maternal factors using machine learning models. *Under review in. IEEE Access.* 2022.

Widatalla N, Alkhodari M, Koide K, et al. Pattern-based assessment of the association of fetal heart rate variability with fetal development and maternal heart rate variability. *Submitted to PLoS ONE.* Jan 2023.

Conference publications:

Widatalla N, Khandoker A, Yoshida C, et al. Effect of valproic acid on maternal - fetal heart rates and coupling in mice on embryonic day 15.5 (E15.5). In EMBC 2021; 2021; Mexico.

Chapter 2: Literature Review

2.1 Brief review of maternal-fetal HR relations

The prenatal period constitutes the period in which a mother is closest to her child. The mother provides the essentials and resources needed for child development and growth by blood through the placenta. Hence, factors associated with the maternal circulatory system, such as blood pressure and HR, are of importance for fetal development. Because the fetus is inaccessible, assessment of fetal development and growth has been carried out by using non-invasive techniques. For example, a Doppler ultrasound or an ear trumpet can be used to listen to fetal heartbeats (16). fHR is a major biomarker for fetal health and well-being, hence, previous research attempted at understanding factors that may potentially affect fHR for a better understanding of fetal development. fHR was found to be associated with maternal condition and HR. For example, the maternal arterial oxygen content was found to affect fHR (17). The physiological pathways by which the mother exerts its influence on fHR are yet to be uncovered and previous studies attempted at understanding them by studying the association between maternal and fetal HR. The association was investigated by adopting different methods that involved, correlation analysis between average maternal and fetal HR and coupling analysis between both HRs. The followings provide a summary of some of the previous studies that addressed maternal and fetal HR association.

Study 1 (18)***:***

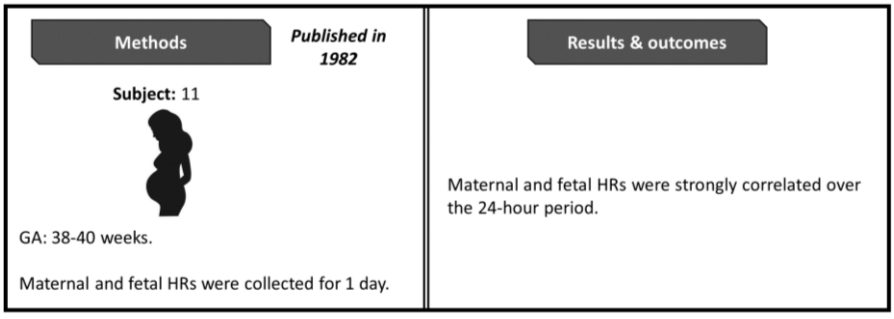

Study 2 (11)*:*

Methods

Published in 1987

Subject: 10

GA: 20-22 weeks.

Device: Hewlett-Packard 803OA

Analysis:
fRRI was recorded on a cardiotocograph strip chart as beats/min for 1 day.

Results & outcomes

fHRs showed diurnal patterns in which they increased at daytime and decreased at night

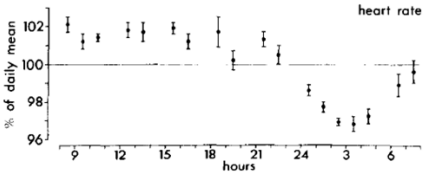

Study 3 (12)*:*

Methods

Published in 1998

Subject: 26

GA: 26 - 33 weeks.

Devices:
Hewlett-Packard M1350A ultrasound HR monitor was used for fHR recording.

Polar sporttester was used for mHR recording.

Analysis:
Average mHR was calculated per 3 minutes for 1 day.

Average fHR was calculated per 3.75 minutes for 1 day.

Results & outcomes

Correlation analysis between maternal and fetal HRs was conducted in 14 subjects and the results showed that positive correlations exist between both. Correlation coefficients ranged between 0.37 and 0.89.

Maternal and fetal HRs showed diurnal rhythm.

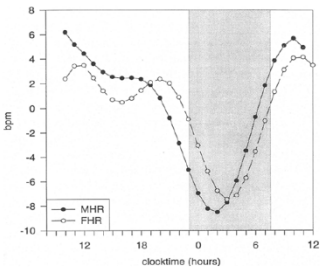

Fig. 4. Mean "best fits" of mean maternal heart rate *(MHR)* and mean fetal heart rate *(FHR)* in 14 pregnancies. Dashed area indicates the night period, during which lights were off.

Study 4 (19)*:*

Methods

Published in 2003

Subject: 62

GA: 16-42 weeks.

Device: 61 channel biomagnetometer (Magnes 1300C, 4D-Neuroimaging, San Diego).→ To capture maternal and fetal MCG.

Analysis:
MCG records were collected for 5 minutes.

Synchrograms were constructed by using the stroboscopic technique → phases of fetal R peaks were plotted with respect to maternal cycles.

Results & outcomes

Occasional coupling between maternal and fetal heart beats were found. In the below figure, thick black points indicate synchronization epochs.

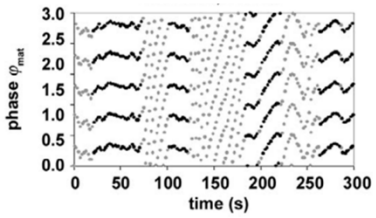

Study 5 (20)*:*

Methods

Published in 2004

Subject: 137

GA: 20-38 weeks.

Devices:
Toitu (MT320) fetal actocardiograph for fHR measurements

Bioamplifier for mHR measurements.

Analysis:
Maternal and fetal measurements were recorded for 30-50 minutes.

Cross correlation between maternal and fetal HRs were performed to quantify coupling.

Results & outcomes

Cross correlation analysis found no temporal associations between maternal and fetal time series HRs → no coupling.

Significant correlations between average maternal and fetal HRs were found during 28 – 38 weeks. Correlation coefficients ranged between 0.13- 0.33 as shown below.

	Gestational age (weeks)					
Variable pair	20	24	28	32	36	38
Maternal heart rate/ fetal heart rate	.13	.14	.17*	.26**	.21**	.33**

* P<0.05. **P<0.01

Study 6 (14)*:*

Methods

Published in 2009

Subject: 6

GA: 34-40 weeks.

Device: Magnes 1300C multi-channel biomagnetometer (4D Neuroimaging) → To capture maternal and fetal magnetocardiography (MCG).

Analysis:
Participants were asked to control their breathing rates at four rates: 10, 12, 15 and 20 cycles per minute (cpm).

6 consecutive 5 minute recordings of MCG were collected to quantify maternal-fetal HR coupling and calculate number of synchronization epochs.

Results & outcomes

The number of synchronization epochs increased with maternal beathing rates.

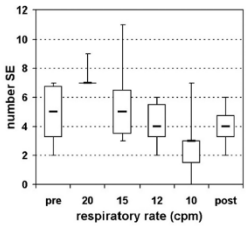

Study 7 (21)*:*

Methods

Published in 2016

Subject: 12

Second half singleton pregnancy:
GA >=36 weeks (n = 5).
GA < 36 weeks (n=7).

Device: Monica AN24

Analysis:
The device measures non-invasive maternal and fetal electrocardiogram (ECG) and it provides data as average HR every 2 seconds.

Data was collected for an average of 1 day.

Results & outcomes

Correlation analysis between maternal and fetal HR per subject revealed the followings:

Maternal and fetal HRs were significantly correlated in 11 subjects (P<0.001), in one subject (GA = 32 weeks), there was no significant correlation, p = 0.22.

Median beta coefficient of the entire cohort was 0.189: GA >= 36 weeks: (0.14 (range: 0.006-0.204)), GA < 36 weeks: 0.347 range (0.106-0.431).

Maternal and fetal HRs showed diurnal patterns in which they decreased at night.

Study 8 (22)*:*

Methods

Published in 2015

Subject: 65

GA: 16-41 weeks.

Device: Iris monitor (Japan)

Analysis:
Simultaneous records of non-invasive maternal and fetal ECG were analyzed for 1 minute to estimate maternal-fetal HR coupling by using transfer entropy (TE).

Maternal respiratory rate was estimated through single lead ECG-Derived Respiration (EDR).

Results & outcomes

TE analysis investigated transfer of information from maternal HR to fetal HR and vice versa. The results showed that maternal to fetal HR transfer increased with GA, however the opposite transfer decreased.

The study found that there was no correlation between maternal respiratory rate and coupling strength that was measured by TE.

Study 9 (23)*:*

Methods

Published in 2018

Subject: 6

ED: 17.5 days

Device: Biomedical amplifier to record maternal and fetal ECG.

Analysis:
Maternal and fetal ECG were recorded for 20 minutes. After the 10th minute, saline or atropine was injected to the mother (3 mice were injected with saline and the other 3 were injected with atropine). After that, maternal-fetal HR coupling was quantified pre and post injection. Coupling was estimated by using sycnhrogram and phase coupling index (λ).

Results & outcomes

Atropine injection affects maternal-fetal HR coupling patterns.

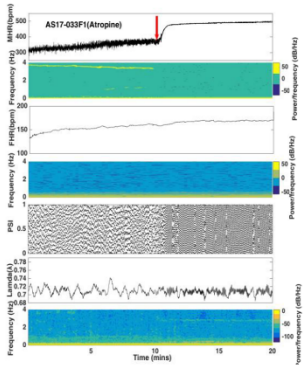

Study 10 (6)*:*

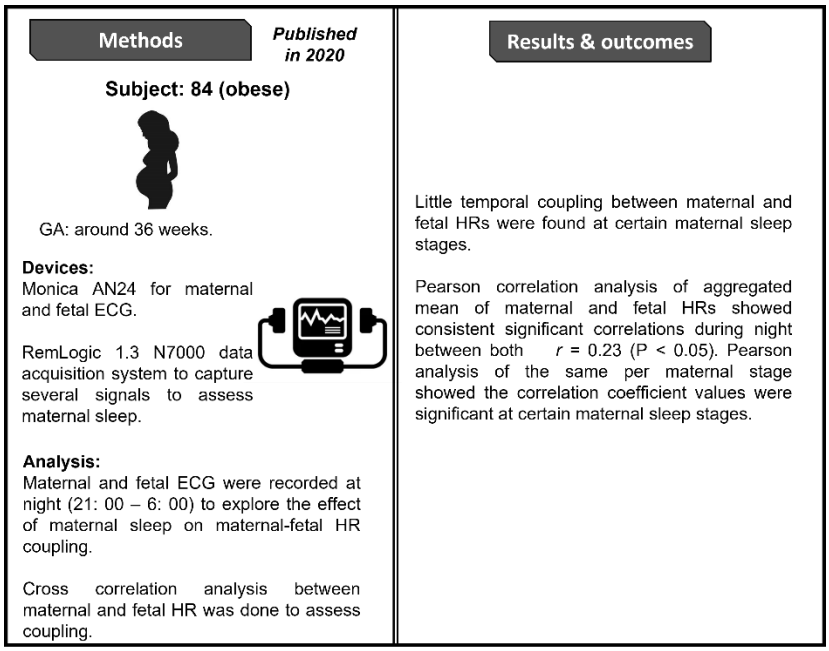

The previously mentioned studies (study 1 - study 10), attempted at understanding the relationship between maternal and fetal HRs. In some studies, an intervention was done for a better understanding of maternal-fetal HR coupling or association. For example, in study 6, the participants were asked to control their breathing to see how maternal-fetal HR coupling changes. In study 9, mice were injected with atropine to study the same changes. Although previous studies showed that coupling or synchronization occurs between maternal and fetal HRs, up until now, the correlation between both HRs remains ambiguous. The latter is attributed to the discrepancies among the previously mentioned literature regarding the presence of a correlation between maternal and fetal HRs. For example, in study 5, significant correlations between the average maternal and fetal HRs were found at certain GAs only. Also, cross-correlation (CC) analysis showed there were no time series correlations between both. In study 9, significant correlations between average HRs were found at certain maternal sleep stages only. With respect to time series correlations in study 10, they were found at certain maternal stages as well. Hence, based on the previous studies, the question regarding when do mHRs correlate or associate with fHRs remains.

In study 6, *Leeuwen et al.* (14) found that synchronization epochs between maternal and fetal HRs were affected by maternal respiratory rates. However, in study 8, *Marzbanrad et al.* (22) found no correlation between maternal respiration and coupling strength. The discrepancies between both studies regarding the effect of respiratory rate could be attributed to the different methods used to quantify coupling. Also, *Marzbanrad et al.* (22) did not control respiration, rather, they used ECG-

derived respiration in their study. The differences between both studies raise the question regarding which method could be reliable in assessing coupling between maternal and fetal HRs. Further, the fact that different time segments were used in both studies brings up further concerns regarding the optimal window size to estimate coupling. It is worth mentioning that the significant correlations that were reported between average HRs in studies # 1, 2, 3, 5, 7, and 10 entailed long-term recordings. Therefore, correlations between average maternal and fetal HRs over the short term remain ambiguous and more studies are needed to clarify this.

In previous studies (study # 5, 6, 10), discussions regarding the cause of maternal-fetal HR coupling were addressed but up until now the cause remains unknown and there is a discrepancy in the literature about the same. For example, *Leeuwen et al.* (14) suggested that maternal-fetal HR coupling occurs due to stimulation of the fetal auditory system by maternal heart beats rhythm. Whereas *Dipietro et al.* (20) argued that maternal-fetal HR coupling occurs due to secondary processes that mediate both HRs.

2.2 Brief review of the relationship between maternal condition and fetal HR or HRV

In addition to studying correlations between maternal and fetal HRs, different studies investigated how maternal health may affect fetal HR and HRV. The following studies addressed the effect of maternal exercise, obesity, and blood pressure (BP) on fetal HR or HRV.

Study 11 (24)*:*

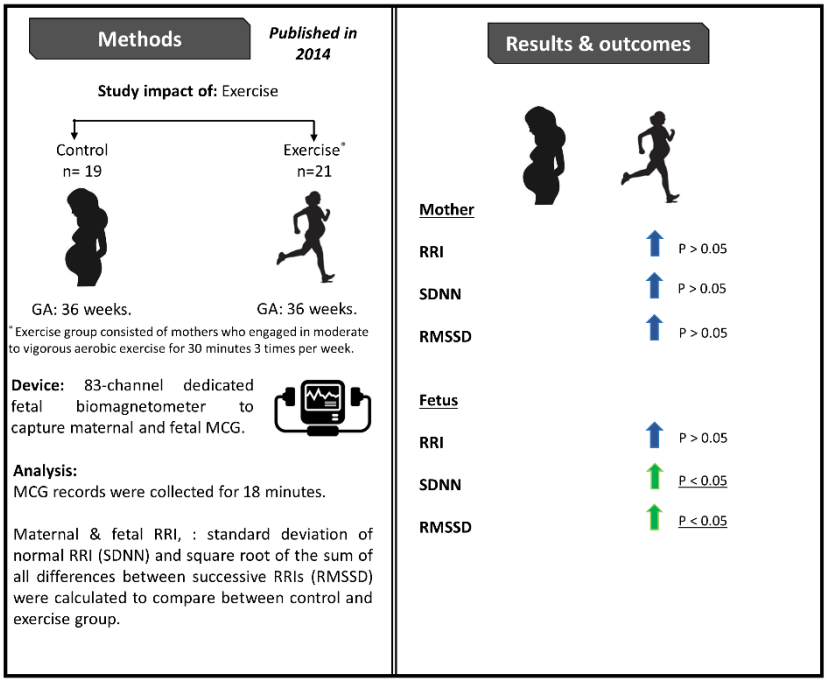

Study 12 (25)*:*

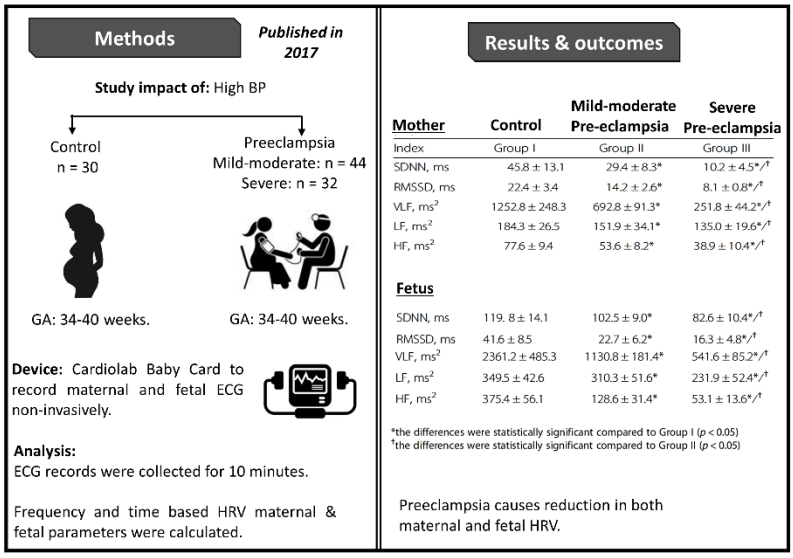

Study 13 (15)*:*

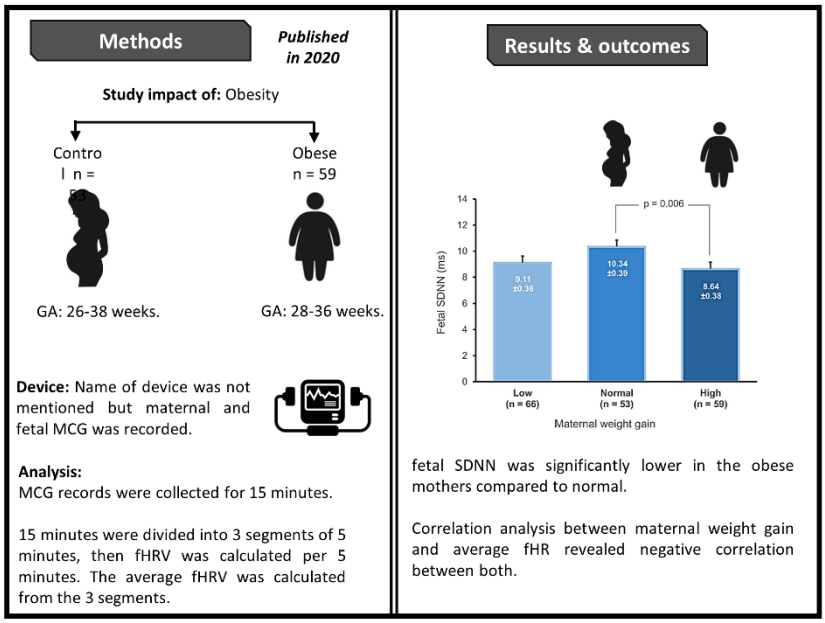

The results from studies 11-13 showed that maternal condition may affect fetal HR or HRV. It is unknown how much deviation from the norm is considered normal or abnormal as more research is needed to define normal ranges for fetal HR and HRV. But, generally, lower fetal HRV was associated with abnormality, for example, Lakhno, I. (26) found that growth-restricted fetuses had lower HRV compared to control (26). According to the DOHaD (4) and Barker's theory (2), understanding changes

in fetal HRV relative to the maternal condition may provide a better understanding of the origin of diseases that are diagnosed during adulthood. The pathways in which a mother exerts her influence on fetal development are yet to be fully explored, and according to (study 1 - study 10), the mechanism by which maternal and fetal HR interacts constitutes one of those pathways.

2.3 Conclusion

Different studies investigated maternal-fetal HRs coupling and up until now, the correlation between both HRs remains ambiguous. Understanding coupling patterns can be used to understand why the maternal condition can affect fetal HR and HRV. Based on study 1 - study 13, major questions can be formulated:

- How average maternal and fetal HR and HRV are correlated over the short term? Are they positively or negatively correlated?

- What is an optimal method to quantify maternal and fetal HR coupling?

- Why does maternal-fetal HR coupling exist? Do they have physiological implications, or do they occur due to fetal auditory response to maternal HRs?

Chapter 3: Maternal-fetal RRI similarity

3.1 Brief overview of the chapter

In Chapter 2, several studies about maternal-fetal HR coupling were discussed. The methods by which maternal-fetal HR coupling was investigated varied among the studies and in all of them, the presence of some sort of coupling between maternal and fetal heartbeats was reported. Conclusions regarding the presence of coupling were made based on:

- Mathematical quantification of synchronization in synchrograms composed of phase-transformed maternal-fetal heartbeats (e.g. study # 4, 6 & 9).
- Mathematical quantification of synchronization between maternal and fetal RRI by using TE (e.g study # 8).
- CC analysis of long recordings of time series maternal and fetal HRs (e.g. study # 5 &10).

Although coupling analysis was performed based on previous assumptions that some sort of coupling exists between maternal and fetal heartbeats, there was a lack of attempts at exploring the possibility of finding similarities between maternal and fetal RRI over the short term. In our research, we performed a visual inspection of simultaneous records of maternal and fetal RRI tachograms and we found that there were obvious similarities between both. To understand their physiological implications, we quantified them based on CC analysis, then we investigated the correlation between the CC coefficients and GA. Also, we investigated the correlations between CC coefficients and maternal and fetal HRV. Figure 1 provides an illustrative summary of the methods and results discussed in this chapter.

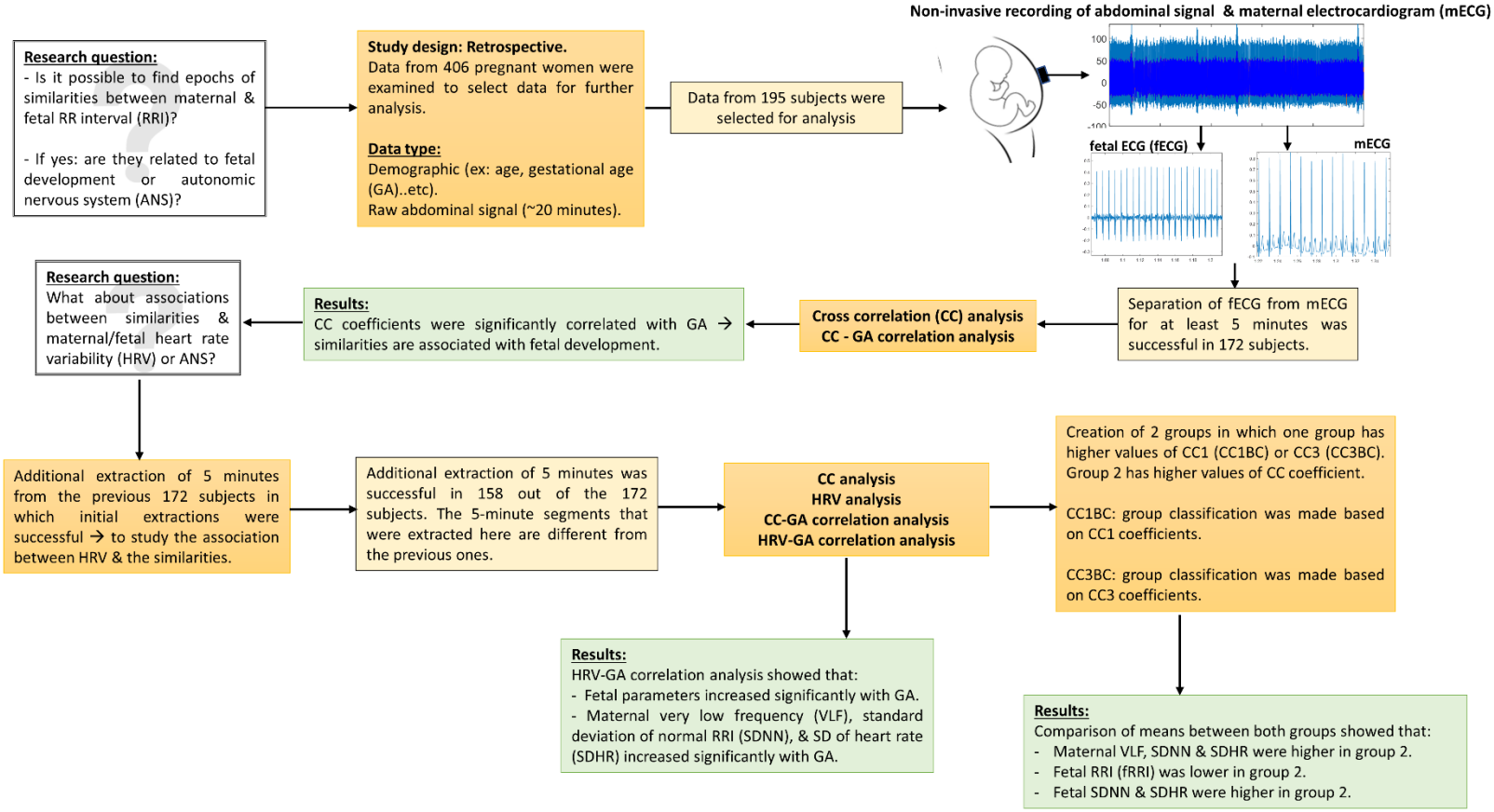

Figure 1: Illustrative summary of chapter 3

3.2 Methods

3.2.1 Data Collection

The study described in this manuscript was approved by the Tohoku University Institutional Review Board (Approval number: 2021-1-133). A total of 406 outpatient or in-patient pregnant women (GA: 19-40 weeks), who visited Tohoku University Hospital, Japan, for antenatal checkups or treatment of pregnancy-related illnesses, were recruited during 2009-2019 for different projects that were carried out at Tohoku University. The women were recruited after getting their informed consent. The 406 sample size reflects the number of participants who were recruited from among all pregnant women who visited the Tohoku University Hospital. Pregnant women who were recruited were at least 20 years old and could read and understand the written informed consent in Japanese.

Before recruiting the participants, an obstetrician confirmed the schedule and location of the ECG measurements. Then a subject who met the selection criteria, mentioned above, was approached for recruitment after informing her about the research details and ECG measurements. Demographic data of the participants were collected such as age, height, and weight. Information regarding maternal health and medication along with fetal weight and health were recorded. Participants were asked to remain in a supine position and 12 electrodes were attached to their abdominal surface to obtain simultaneous records of non-invasive maternal and fetal ECG records. 10 of the 12 electrodes were attached to the maternal abdomen to capture fECG. The other two electrodes were attached to the back and right thoracic position. The electrode that was attached to the back is the reference electrode and the thoracic electrode was used to capture maternal ECG (mECG). The signals were recorded with a 1 kHz sampling frequency and 16-bit resolution (27). Signals' recordings lasted for 20-min. In this study, we analyzed data retrospectively.

3.2.2 Data selection and fetal ECG (fECG) extraction

The exclusion criteria for this study entailed: 1) fetuses who had records of medical complications when ECG data were collected, and 2) subjects with missing information regarding GA or fetal or maternal health. The total number of data that met the exclusion criteria was 211, hence, around 195 data were considered for analysis in this study.

Extraction of fECG from mECG was conducted by using a MATLAB 2008b code. The code extracts fECG based on blind source separation with reference (BSSR) which is described in detail in (28). fECG

extraction was performed for at least 5-mins per subject. No particular procedures were followed to assess the quality of the raw abdominal signals to select a 5-min segment for fECG extraction. A signal's quality was considered good if the software was able to extract clear fECG signals. Clear fECG signals made fetal R peak detection easy. A window size of at least 5-min was chosen mainly to accommodate for the very low frequency (VLF) band (0.0033 - 0.04) Hz. Due to technical limitations related to the quality of the raw abdominal signals, it was difficult to perform analysis on more than 5-min lengths.

fECG extraction attempts were carried out in chronological order. Hence, fECG extractions were done starting from the beginning of the ECG records, if the software failed to extract fECG from the selected segments, extractions of the next 5-min segments were attempted. If the extraction was not successful in any 5-min segment, the data were excluded. As a result of the latter steps, fECG signals were extracted at the beginning, middle, or end of the recording.

In the initial extraction attempts, the total number of 5-min segments (1 segment per 1 subject) that were extracted from the 195 subjects was 172 (age: 22-45 years old (34 ± 5.3), GA: 19-40 weeks (30 ± 6.1). Extraction of fECG from the rest of the 23 subjects was not possible due to noise (e.g maternal myoelectric and environmental noise). After analysis of the 172 segments, an additional 5-min segments were extracted to get more insights into the similarity between maternal and fetal RRI and its correlation with HRV. Extraction of additional segments of 5-min was possible in 158 cases (age: 22-44 years old (34 ± 5.3), GA: 19-40 weeks (30 ± 6.2)). With the second fECG extraction, the total number of 5-min segments extracted per subject was two in 158 subjects. The additionally extracted 5-min segments did not overlap with the previously extracted segments. Extraction of two segments of 5-min from all 172 subjects was not possible due to noise in the data, also, around three data sets had recordings of less than 10 mins. Around 44 pregnant women had no records of medical or obstetric complications, however, the rest of the subjects had at least one complication, more details are found in Appendix A.

3.2.3 Similarity quantification with CC analysis

- RRI and HRV calculation

To investigate the presence of similarity between maternal and fetal RRI tachograms and further investigate the similarity's association with fetal development, we calculated RRI and HRV. To obtain RRI tachograms from ECG, R peaks were detected by using the "findpeaks" function in MATLAB 2020b and the code is described in (29) and Appendix B, detected R peaks were verified visually to ensure that the

code detected R peaks only, an example of detected R peaks is demonstrated in Appendix C. R peaks were detected in maternal and fetal ECG signals which were captured at 1 kHz. The "findpeaks" function detects peaks based on a threshold value, here the threshold value was adjusted based on the R peak amplitudes that varied among subjects. The "findpeaks" provides the location of the detected peaks along with their amplitudes. Following R peak detections, the time difference between two successive R peaks was calculated to obtain RRI signals or RRI tachograms. By using RRI, maternal and fetal HRV parameters were calculated.

Time and frequency-based HRV analysis was performed in MATLAB. For HRV analysis, original non-resampled RRI data was used and abnormal sinus RRI values were corrected manually by replacing them with preceding or subsequent RRI values. Time-based HRV analysis entailed calculations of the average RRI, standard deviation (SD) of normal RRI (SDNN), and SD of HR (SDHR). Frequency-based analysis was done by using the Lomb-Scargle periodogram with considering the following bands:

mECG: VLF: (0.0033 - 0.04) Hz, LF: (0.04 - 0.15) Hz, high frequency (HF): (0.15 - 0.4) Hz.

fECG: VLF (0.0033 - 0.03) Hz, LF: (0.03 – 0.2) Hz, HF (0.2 - 2) Hz.

mECG bands were chosen based on previously defined bands for human adults (30). Since up until now there are no well-defined bands for fECG, we used bands that were used for infants (31,32).

- *Similarity trend analysis*

To check for the presence of similarity epochs, the values of RRI signals were normalized by using *Eq. 1*:

$$Normalized\ RRI = \frac{RRI - mean\ RRI}{\max(RRI - mean\ RRI)} \quad Eq.1$$

After normalization, maternal and fetal RRI tachograms were plotted together in one panel to visualize the similarities between maternal and fetal RRI tachograms.

- *Cross-correlation (CC) coefficient calculation*

To obtain a similarity score or a mathematical measure of the similarity, we performed CC analysis in MATLAB 2020b. CC analysis measures the similarity between two signals at different time lags, more details can be found in (33). The CC coefficients of two signals *f* and *g* are calculated by using Eq. 2.

$$f \star g = \int_{-\infty}^{\infty} f^*(t)\ g(\tau + t)\, d\tau \qquad \text{Eq.2}$$

$f^*(t)$ is the complex conjugate of *f (t)* and makes no difference if the signal is a real-valued (34).

Due to the difference in the range of maternal and fetal RRI values, the number of maternal RRI samples per 5-min segment was lower than that of the fetus. Hence, to unify the lengths of maternal and fetal RRI signals per 5-min segment, we resampled both at 0.5 Hz. Resampled RRI signals were calculated by taking the average of RRI per 2 seconds. Resampling per 2 seconds (2000 samples) yields a signal with 150 samples for a 5-min signal (300,000 samples), $\frac{300{,}000}{2000} = 150$.

An example of a resampled signal is demonstrated in Figure 2, Appendix C provides more information about resampling. Resampled maternal and fetal RRI signals were then normalized per subject by using *Eq.1*.

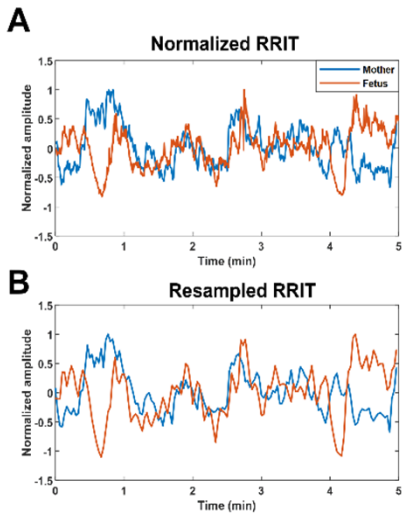

Figure 2: Example of a resampled signal. (A) Original maternal and fetal RR interval (RRI) tachograms. (B) Resampled RRI tachograms. Resampling was done by taking the average of RRI per 2 seconds.

After resampling and normalization, the resampled RRI signals (with 150 samples) were divided into 15 segments to calculate CC. CC coefficients were calculated per 10 samples by using the "xcorr" function in MATLAB; CC values were calculated with a zero-time lag. We opted for calculating CC per 10 samples rather than the whole 150 samples to capture transient changes in the similarity. CC analysis of the whole resampled RRI signal (150 samples) may lead to an underestimation of the similarity. Next, the overall similarity per case (5-min segment) was estimated by taking the average of the 15 coefficients. Here, we adopted four different methods to estimate the overall similarity. We used different methods for CC coefficient calculations because, so far, it is unknown what could be a good way to quantify similarity to get insights into fetal development. We calculated our four CC coefficients as follows:

CC1: this coefficient was calculated by taking the absolute average of the 15 coefficients as given by Eq. 3 (CC1 is not normalized). CC1 provides a rough score for the similarity, the higher the CC1 value is, the higher the degree of similarity between maternal and fetal RRI.

$$CC1 = \frac{|X_1 + X_1 \ldots\ldots\ldots\ldots + X_{15}|}{15} \quad \text{Eq. 3.,} \quad \text{X indicates the CC coefficient of 10 samples}$$

CC2: this coefficient was calculated by taking the non-absolute average of the 15 coefficients as indicated in Eq. 4 (CC2 is not normalized). CC2 quantifies the similarity between maternal and fetal RRI by considering directionality (whether maternal and fetal RRIs are changing in the same or opposite

directions). Since CC2 is a non-absolute mathematical average of 15 CC coefficients, the sign of the CC2 value reflects the dominant similarity trend, positive or negative, within a 5-min segment.

$$CC2 = \frac{X_1 + X_1 \ldots\ldots\ldots\ldots\ldots + X_{15}}{15} \quad \text{Eq. 4,} \quad \text{X indicates the CC coefficient of 10 samples}$$

CC3: to calculate this coefficient, the "normalized" option of the "xcorr" function was applied in MATLAB when the 15 coefficients were calculated. After that, the absolute average of the 15 coefficients was calculated by using Eq. 5. The meaning of CC3 is similar to that of CC1.

$$CC3 = \frac{|X_1 + X_1 \ldots\ldots\ldots\ldots\ldots + X_{15}|}{15} \quad \text{Eq. 5,} \quad \text{X indicates the CC coefficient of 10 samples}$$

CC4: the 15 coefficients were calculated similarly to CC3 (with the "normalized" option in MATLAB), then the non-absolute average of the 15 coefficients was calculated by using Eq. 6. The meaning of CC4 is similar to that of CC2.

$$CC4 = \frac{X_1 + X_1 \ldots\ldots\ldots\ldots\ldots + X_{15}}{15} \quad \text{Eq. 6,} \quad \text{X indicates the CC coefficient of 10 samples}$$

A summary of CC1, CC2, CC3, and CC4 calculations is provided in Appendix D, also the MATLAB code that was used to resample RRI signal and perform CC analysis is provided in Appendix E. We performed a brief comparison among our derived coefficients based on their potential linkage to fetal development. The linkage was assessed by performing a linear correlation analysis between the CC coefficients and GA.

3.2.4 Data classifications based on CC1 and CC3

To get more physiological insight into the similarity between maternal and fetal RRI, we made two groups by using the 2 extracted segments of 5-min (from the 158 subjects) to compare their HRV features. The comparison analysis was carried out twice. In the first comparison, the data were classified based on the CC1 coefficient (CC1-based classification (CC1BC)) and in the second comparison, data were classified based on the CC3 coefficient (CC3-based classification (CC3BC)). Group 2 had higher values of CC1 or CC3 compared to group 1. The main purpose of this analysis is to see if there will be significant differences in HRV between the two groups due to the effect of CC1 or CC3. Figure 3 shows a summary of data extraction and CC classification.

Here, we based our classification on CC1 and CC3 only because, mathematically, they provide a stronger measure for the overall similarity between maternal and fetal RRI compared to CC2 and CC4. In CC2 and CC4, similarity quantification by using CC analysis might be underestimated due to the mathematical

summation of negative and positive numbers. Also, data classification based on CC2 and CC4 was not done due to the complexity involved in the classification and interpretation of the results (more details are found in the discussion).

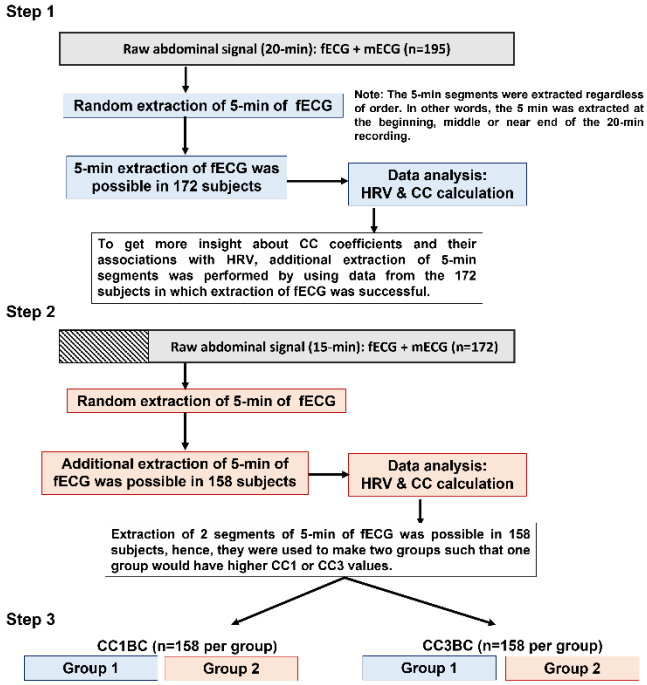

Figure 3: Summary of data analysis. The flowchart provides a graphical summary of the steps that were followed to analyze the data. In Step 1, 5-minutes (mins) extraction of fetal electrocardiogram (fECG) was successful in 172 out of 195 subjects. In step 2, additional extraction of 5-min segments was successful in 158 out of the 172 subjects. Both in step 1 and step 2 cross-correlation (CC) and maternal and fetal heart rate variability (HRV) analyses were performed for the extracted 5-min segments. In step 3, a comparison of means analysis was performed to compare between group 1 and group 2 in terms of maternal and fetal HRV analysis. Group 2 has higher CC1 or CC3 values compared to group 1.

3.2.5 Statistical analysis

Normality tests were conducted in MALTAB 2020b by using the One sample Kolmogorov-Smirnov test (kstest) and the Shapiro-Wilk test (swtest) (35). Kstest revealed that all variables were non-normally distributed regardless of group. On the other hand, swtest revealed that some variables were normally distributed in both groups (group 1 and group 2), and others were normally distributed in one group only. Hence, we based our normality tests on the kstest only.

Correlation analysis between two variables was performed by using the spearman test.

Comparison of means was performed by using the Friedman test.

3.3 Demonstration of maternal-fetal RRI tachogram similarities

Maternal and fetal RRI tachograms were found to exhibit positive and negative similarity trends. In a positive similarity trend (Figure 4 A, B, and C (A-C)), maternal and fetal RRI tachograms change in the same direction. In Figure 4A, it is noticeable that the LF and VLF oscillations exhibited by fRRI are similar to that of the maternal RRI (mRRI). In Figure 4B, fetal and maternal RRI increased in synchrony before the 1st min, and then, they decreased but with a time lag at around the 2nd min. Similarities between maternal and fetal RRI tachograms were found to exhibit time lags as demonstrated in Figure 4C over the period 2.7 – 4 min.

In negative similarity trends, maternal and fetal RRIs change in opposing directions (Figures 4 D, E and F (D-F)). The upper panels in Figures 4D-F show the original normalized RRI tachograms and the lower panels show the same but with the maternal signal inversed. After inversing maternal RRI tachograms, the similarities between maternal and fetal RRI tachograms are clearer. In Figure 4D, the increase in fRRI at around the 1st min was accompanied with a decrease in mRRI but with a time lag, the latter is made clearer in the lower panel after inversing the maternal signal. Another example of a negative similarity trend is demonstrated in Figure 4E. In Figure 4F, RRIs are changing in opposing directions over the period 0 - 3.5 min, however, the trend changes to positive afterward.

3.4 Similarities' association with fetal development

We hypothesized that the similarities between maternal and fetal RRI tachograms that were demonstrated in Figure 4 could be associated with fetal development. Hence, we opted for obtaining mathematical measures for the similarity by using CC analysis in which we obtained four coefficients, CC1, CC2, CC3, and CC4. The linear correlation between the four coefficients and GA was calculated to investigate the association of similarity with fetal development. The results of this analysis are shown in the upper rows of Table 1 (the correlation coefficient with GA is represented as *r*). For further investigation, we calculated the linear correlations between fHRV and GA and between maternal (mHRV) and GA. The mean, SD, median, and ranges of HRV parameters along with their correlations with GA are shown in Table 1.

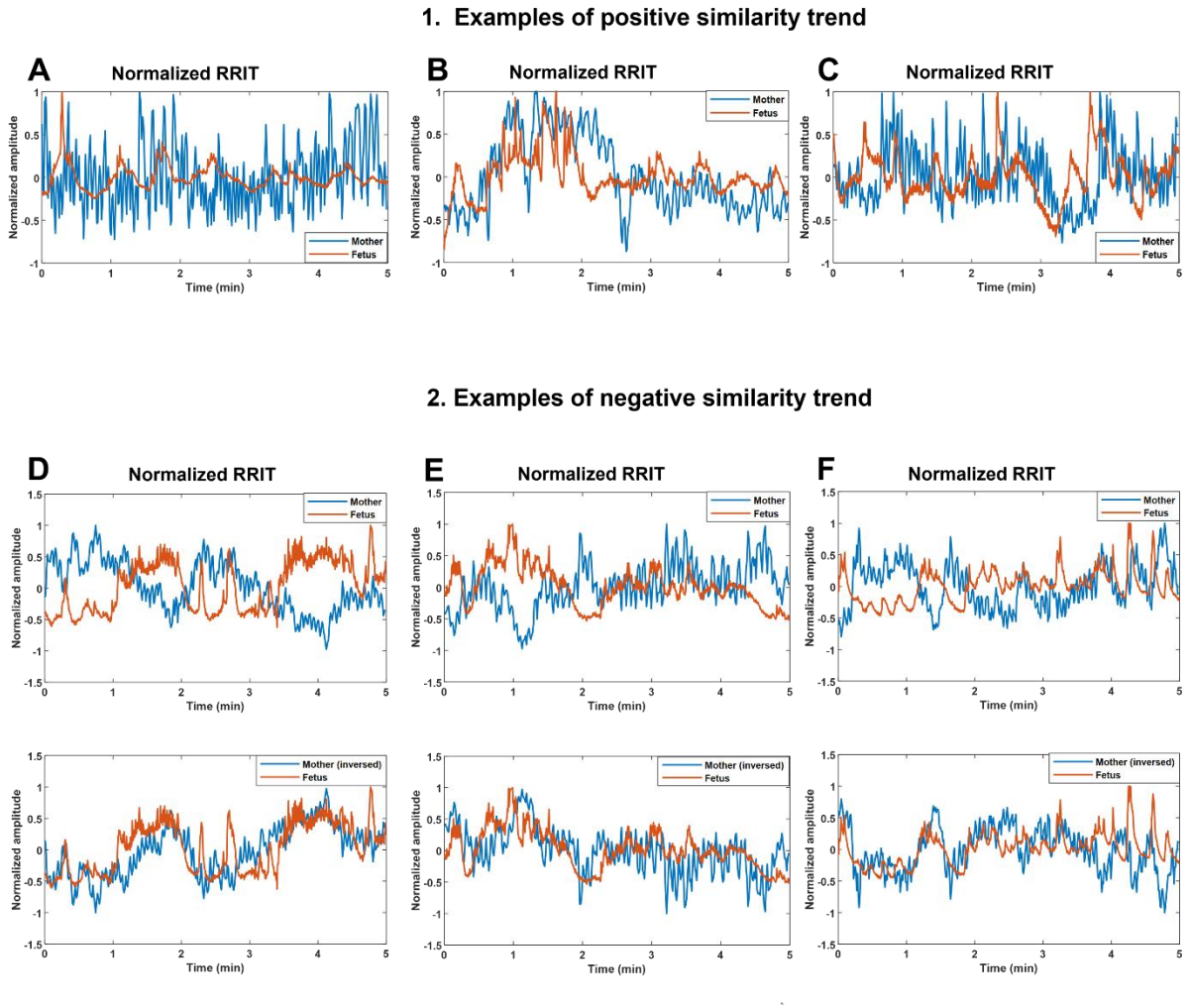

Figure 4: Demonstration of positive and negative similarity trends between maternal and fetal RR interval (RRI) tachograms. Figures A, B, and C (A-C) show examples of positive similarity trends in which maternal (blue) and fetal (orange) RRI tachograms change in the same direction. Figures D, E and F (D-F) show examples of negative similarity trends in which maternal and fetal RRI tachograms change in opposing directions. The upper panels in Figures D-F show the original signals while the lower panels show the original fetal signal with the maternal signal inversed. (A) The record belongs to a mother who had no records of medical complications, gestational age (GA): 20 weeks. (B) The record belongs to a mother with a record of uterine/appendix disease, GA: 23 weeks. (C) The record belongs to a mother with a medical record of respiratory disease and uterine/appendix disease, GA: 20 weeks. (D) The record belongs to a mother with a medical record of autoimmune disease, gestational age (GA): 39 weeks. (E) The record belongs to a mother who had a blood disease, GA: 33 weeks. (F) The record belongs to a mother with no records of medical complications, GA: 23 weeks.

Among the four CC coefficients, CC1 was found to have the highest significant correlation with GA where *r* = 0.40 (Table 1). At advanced GA, it was revealed that the negative similarity trend prevails, and this is indicated in CC2 and CC4 with *r* values of - 0.26 and - 0.20, respectively (Table 1). The results of fHRV - GA correlation analysis showed that there was a significant increase in the associations of fetal HRV and RRI with GA, (Table 1). The mHRV - GA correlation analysis showed that mHRV, VLF, SDHR, and SDNN were significantly correlated with GA (Table 1). Also, LF was found to be significantly correlated with GA but with a lower *r* value compared to VLF, SDHR, and SDNN (Table 1).

Table 1: Summary of maternal and fetal HRV, CC coefficients and their correlations with GA, n=172.

Feature	Correlation between CC coefficients and GA		
	median (min – max)	(mean ± SD)	*r*
CC1	0.58 (0.11 – 2.5)	0.63 ± 0.32	0.40†
CC2	- 0.023 (-1.3 – 0.80)	- 0.09 ± 0.36	- 0.26†
CC3	0.43 (0.21 – 0.71)	0.44 ± 0.10	0.19*
CC4	- 0.012 (-0.53 – 0.49)	- 0.03 ± 0.18	- 0.20†

Feature	Correlation between HRV and GA			
	Maternal Features		Fetal features	
	(mean ± SD) median (min-max)	*r*	(mean ± SD) median (min-max)	*r*
RRI (ms)	760 ± 113 742 (530 – 1125)	- 0.03	412 ± 25 409 (354 – 512)	0.33†
SDNN (ms)	35 ± 14 31 (13 – 87)	0.35†	16 ± 6.9 15 (4.0 – 36)	0.56†
SDHR (bpm)	3.7 ± 1.4 3.5 (1.5 – 8.9)	0.39†	5.7 ± 2.5 5.2 (1.6 – 14)	0.49†
VLF (Ln)	6.2 ± 0.76 6.2 (4.1 – 8.2)	0.45†	4.5 ± 1.1 4.6 (1.8 – 6.8)	0.52†
LF (Ln)	5.1 ± 0.80 5.1 (3.3 – 7.7)	0.16*	4.3 ± 0.85 4.4 (1.4 – 6.1)	0.53†
HF (Ln)	4.7 ± 1.3 4.7 (1.1 – 7.8)	0.10	2.3 ± 0.81 2.4 (-0.46 – 4.2)	0.53†

*** P < 0.05, † P <0.005, HRV: heart rate (HR) variability, GA: gestational age, CC: cross-correlation, RRI: RR interval, SD: standard deviation, SDNN: SD of normal RRI, SDHR: SD of HR, bpm: beats per minute, VLF: very low-frequency power, LF: low-frequency power, HF: high-frequency power, *r*: spearman correlation coefficient.**

3.5 Similarities' association with HRV

We aimed at investigating how HRV is associated with the similarity (or CC coefficients) to identify mechanisms or physiological pathways that could be associated with the same similarity. Hence, we extracted additional 5-min segments to make two groups such that one group would have a higher similarity score or a CC coefficient value compared to the other group. As was mentioned in the methods section, we made two groups based on CC1 (CC1BC) and CC3 (CC3BC) to compare group 1 and group 2. After classifying the data based on CC1 and CC3, the correlation analysis in (Table 1] was repeated, CC1BC results are shown in (Table 2). CC3BC provided similar results (see Appendix F). A comparison of group 1

and group 2 in the terms of the association of fHRV with GA revealed that the *r* values were found to be higher in group 2 compared to group 1 (Table 2). Also, comparison between group 1 and group 2 revealed that maternal LF was found to be non-significantly related to GA in group 1 (Table 2).

We conducted comparison of means tests to compare group 1 with group 2 twice, one comparison was based on CC1BC and the other was based on CC3BC, the results of the comparison are shown in Table 3 (CC1BC in Table 3 shows the same CC and HRV values as Table 2). The results of the comparison between group 1 and group 2 showed that there were no significant differences in CC2 and CC4 (Table 3). Maternal VLF and SDNN were found to be significantly higher in group 2 compared to group 1 in both CC1BC and CC3BC (Table 3). SDNN is known to be significantly correlated with VLF (36), hence, the significance observed in SDNN could be largely attributed to VLF. Maternal SDHR was found to be significantly higher in group 2 in the CC3BC.

With respect to fHRV, generally, there were less significant differences between group 1 and group 2. In CC3BC, fRRI was found to be significantly lower in group 2, whereas fetal SDNN and SDHR were found to be significantly higher in group 2.

Table 2: Comparison between group 1 and group 2 in terms of HRV and CC association with GA, n=158

	Group 1 (Low CC1)				**Group 2 (High CC1)**			
Feature	**Correlation between CC coefficients and GA**							
	median (min – max)		(mean ± SD)	*r*	median (min – max)		(mean ± SD)	*r*
CC1	0.43 (0.11 – 1.3)		0.47 ± 0.22	0.44†	0.67 (0.19 – 2.8)		0.72 ± 0.36	0.41†
CC2	- 0.042 (- 0.86 – 0.81)		- 0.064 ± 0.24	- 0.21†	- 0.035 (-1.8 – 1.2)		- 0.10 ± 0.43	- 0.16*
CC3	0.40 (0.21 – 0.69)		0.41 ± 0.09	0.07	0.45 (0.22 – 0.71)		0.46 ± 0.09	0.17*
CC4	- 0.045 (- 0.45 – 0.34)		- 0.044 ± 0.15	- 0.18†	- 0.012 (- 0.53 – 0.49)		- 0.021 ± 0.18	- 0.13
Feature	**Correlation between HRV and GA**							
	Maternal Features		**Fetal features**		**Maternal Features**		**Fetal features**	
	(mean ± SD) median (min – max)	*r*	(mean ± SD) median (min – max)	*r*	(mean ± SD) median (min – max)	*r*	(mean ± SD) median (min – max)	*r*
RRI (ms)	762 ± 116 761 (758 – 1125)	- 0.04	412 ± 26 408 (351 – 512)	0.38†	763 ± 115 763 (751 – 1107)	- 0.02	413 ± 24 410 (353 – 510)	0.40†
SDNN (ms)	33 ± 13 30 (10 – 87)	0.24†	15 ± 6.7 14 (4.5 – 35)	0.36†	36 ± 17 31 (13 – 120)	0.29†	16 ± 7.3 15 (4.0 – 45)	0.55†
SDHR (bpm)	3.5 ± 1.4 3.2 (1.3 – 9.2)	0.35†	5.5 ± 2.5 5.0 (1.2 – 14)	0.29†	3.7 ± 1.6 3.5 (1.5 – 11)	0.33†	5.7 ± 2.5 5.3 (1.6 – 14)	0.50†
VLF (Ln)	6.1 ± 0.81 6.1 (3.9 – 7.9)	0.36†	4.3 ± 1.2 4.4 (0.86 – 6.6)	0.30†	6.2 ± 0.80 6.2 (4.1 – 8.6)	0.34†	4.5 ± 1.1 4.6 (2.3 – 7.2)	0.52†
LF (Ln)	5.1 ± 0.80 5.2 (2.6 – 7.2)	0.09	4.3 ± 0.80 4.4 (1.9 – 5.9)	0.37†	5.1 ± 0.81 5.1 (3.3 – 7.7)	0.19*	4.3 ± 0.87 4.3 (1.4 – 6.5)	0.50†
HF (Ln)	4.8 ± 1.3 4.8 (0 – 8.0)	0.05	2.3 ± 0.77 2.3 (0.67 – 4.2)	0.49†	4.8 ± 1.3 4.7 (1.1 – 7.8)	0.10	2.2 ± 0.83 2.3 (-0.46 – 3.9)	0.51†

*** P < 0.05, † P <0.005, HRV: heart rate (HR) variability, GA: gestational age, CC: cross-correlation, RRI: RR interval, SD: standard deviation, SDNN: SD of normal RRI, SDHR: SD of HR, bpm: beats per minute, VLF: very low-frequency power, LF: low-frequency power, HF: high-frequency power, r: spearman correlation coefficient. (The table was made based on the CC1BC data set)**

Table 3 shows that, as expected, there were no significant differences in CC2 and CC4 between group 1 and group 2. In Table 3, maternal VLF and SDNN were found to be significantly higher in group 2 compared to group 1 in both CC1BC and CC3BC. SDNN is known to be significantly correlated with VLF (36), hence, the significance observed in SDNN could be largely attributed to VLF. Maternal SDHR was found to be significantly higher in group 2 in the CC3BC. With respect to fetal HRV, generally, there were less significant differences between Group 1 and Group 2. In CC3BC, fRRI was found to be significantly lower in Group 2, whereas fetal SDNN and SDHR were found to be significantly higher in Group 2.

Table 3: Comparison in means between Group 1 and Group 2 (n=158)

	CC1BC			*CC3BC*		
Feature	**Group 1 median (min – max)**	**Group 2 median (min – max)**	***P* - value**	**Group 1 median (min – max)**	**Group 2 median (min – max)**	***P* - value**
CC1	0.43 (0.11 – 1.3)	0.67 (0.19 – 2.8)	*P* < 0.01	0.47 (0.11 – 1.3)	0.58 (0.15 – 2.8)	*P* < 0.01
CC2	- 0.042 (- 0.86 – 0.81)	- 0.035 (-1.8 – 1.2)	0.87	- 0.032 (- 0.10 – 0.81)	-0.086 (-1.8 – 1.2)	0.11
CC3	0.40 (0.21 – 0.69)	0.45 (0.22 – 0.71)	*P* < 0.01	0.38 (0.21 – 0.65)	0.48 (0.27 – 0.71)	*P* < 0.01
CC4	- 0.045 (- 0.45 – 0.34)	- 0.012 (- 0.53 – 0.49)	1	- 0.016 (- 0.39 – 0.41)	-0.030 (- 0.52 – 0.49)	0.43
Maternal Features						
RRI (ms)	761 (758 – 1125)	763 (751 – 1107)	0.42	751 (537 – 1125)	757 (530 – 1107)	1
SDNN (ms)	30 (10 – 87)	31 (13 – 120)	0.026	30 (10 – 76)	33 (13 – 120)	0.039
SDHR (bpm)	3.2 (1.3 – 9.2)	3.5 (1.5 – 11)	0.17	3.2 (1.3 – 11)	3.6 (1.3 – 9.4)	0.031
HF (Ln)	4.8 (0 – 8.0)	4.7 (1.1 – 7.8)	0.13	4.7 (0 – 7.8)	4.7 (1.1 – 8.0)	0.81
LF (Ln)	5.2 (2.6 – 7.2)	5.1 (3.3 – 7.7)	0.17	5.0 (2.6 – 7.5)	5.1 (3.3 – 7.8)	0.69
VLF (Ln)	6.1 (3.9 – 7.9)	6.2 (4.1 – 8.6)	0.011	6.0 (3.9 – 8.0)	6.3 (4.1 – 8.6)	0.003
Fetal Features						
RRI (ms)	408 (351 – 512)	410 (353 – 510)	0.87	411 (358 – 512)	407 (351 – 510)	0.002
SDNN (ms)	14 (4.5 – 35)	15 (4.0 – 45)	0.20	14 (4.0 – 45)	15 (4.5 – 36)	0.034
SDHR (bpm)	5.0 (1.2 – 14)	5.3 (1.6 – 14)	0.94	5.0 (1.2 – 14)	5.3 (1.7 – 14)	0.002
HF (Ln)	2.3 (0.67 – 4.2)	2.3 (-0.46 – 3.9)	0.81	2.4 (-0.46 – 4.1)	2.2 (0.46 – 4.2)	0.81
LF (Ln)	4.4 (1.9 – 5.9)	4.3 (1.4 – 6.5)	0.87	4.3 (1.4 – 6.3)	4.4 (1.6 – 6.5)	0.52
VLF (Ln)	4.4 (0.86 – 6.6)	4.6 (2.3 – 7.2)	0.63	4.3 (0.86 – 7.2)	4.6 (1.8 – 6.8)	0.11

CC: cross-correlation, CC1BC: CC1 based classification. CC3BC: CC3 based classification. SD: standard deviation, RRI: RR interval, SDNN: SD of normal RRI, SDHR: SD of heart rate, VLF: very low-frequency power, LF: low-frequency power, HF: high-frequency power.

3.6 Discussion and physiological implications

In this chapter, similarities between maternal and fetal RRI tachograms were demonstrated. Similarities were found to be associated with fetal development by means of correlation analysis between CC coefficients and GA (Table 1). We showed that similarities can be positive (Figure 4A-C), negative (Figure 4D-F) and they may occur with a time lag. We speculate that the similarities arise due to physiological processes regulated by the placenta such as oxygen and nutrition transfer. The presence of similarity suggests that coordination between the mother and her child should exist for proper perfusion

and exchange of blood supply through the placenta**.** The placenta is known to grow with GA, hence, regulations occurring within and affecting maternal and fetal HRs are expected to grow as well due to an increase in blood volume and fetal demand (37).

Due to the limited knowledge in the field, it is difficult to fully interpret the physiological differences between negative and positive similarities and this needs further research, but we believe that they could be related to fetal behavioral states and the typical fetal development cycle. fHRV is known to change with fetal behavioral states and the same states were found to change throughout gestation (38,39). Before 32 weeks of gestation, fetal activity has been classified into two states only which are activity and quiescency or resting (39). In contrast, after 32 weeks of gestation, fetal activity was classified into four states which are: quiet sleep 1F, active sleep 2F, quiet awake 3F, and active awake 4F. In addition to fetal activity, negative and positive epochs could be related to the typical development cycle of fetal ANS. At early GA (<30 weeks), we expect the fetus to be more dependent on the mother for fHRV entrainment and ANS development. With fetal growth, the fetal dependency on the mother is expected to decrease and this may explain the increase in negative similarity epochs at advanced GA.

Table 1 shows that fRRI and HRV increase with GA which indicates fetal development, our results are consisted with previous studies (7,40). The table shows among the mHRV features, only the maternal VLF, SDHR and SDNN increased significantly with GA. An increase in VLF with GA in pregnant women was also reported in previous studies (41,42,43). The increase in VLF with GA highlights its association with the regulation causing the similarity which is further confirmed by the results in Table 3 in which it is shown that mVLF values are significantly higher in group 2 in both CC1BC and CC3CB. The physiological explanation of the VLF in pregnant women received little attention in previous literature. Also, in non-pregnant adults, VLF is considered less defined compared to HF and LF (44). The power within the VLF is believed to be associated with hormonal-related effects since they changed due to angiotensin-converting enzyme (ACE) inhibition (45,46) and thermoregulation (47,48). Similarly, we expect that the VLF in pregnancy could be associated with hormones critical for pregnancy-related regulations. As was mentioned before, the regulations are likely to be connected to the placenta.

The placenta lacks autonomic or neuronal innervations, hence, the prefusion of blood through the umbilical cord is believed to be regulated by placental hormones (37). Blood perfusion through the placenta and umbilical cords depends on vascular resistance and pressure (49), and the regulation that causes the similarity may play a role in controlling them. Identifications of exact hormones that mediate maternal and fetal HRs simultaneously is elusive and more research is needed. However, we expect that

estrogen could be related to the regulation that causes the similarity and mVLF because estrogen is known to be secreted by the placenta and it increases with pregnancy weeks and peak in the third trimester (50). Moreover, estrogen was found to play a critical role in the downregulation of ACE and upregulation of ACE 2 (51,52,53), ACE 2 promotes vasodilation whereas ACE promotes vasoconstriction (54). Previously, it has been reported that inhibition of ACE increased VLF (45,46), hence, the increase in VLF in our study could be related to the increase in estrogen, upregulation of ACE 2 and decrease in ACE, but more research is needed to confirm this.

The similarities between maternal and fetal RRI imply that abnormal changes inflicted in the maternal cardiovascular system may eventually be reflected in fetal HRV and development, therefore, studying them is potentially critical for the assessments of fetal development, and pregnancy and birth outcomes. Understanding the patterns associated with the similarities may help uncover the causes behind some of the cardiovascular diseases that are believed to be related to the maternal uterine environment (4). Also, the presence of regulation that causes the similarity suggests the need for developing clinical biomarkers based on both maternal and fetal HRs.

According to the results in Table 2, it is implied that the similarities may impact evaluations of fetal development based on short-term fetal RRI and HRV as the *r* values between both groups were different. Also, in Table 3, there were differences in fetal RRI, SDRR, and SDHR between both groups in CC3BC. Table 2 shows that there were discrepancies between CC1 and CC3 in terms of differentiating fetal HRV parameters and RRI and this implies that different parameters are being measured by them. However, such differences do not negate the fact that similarities impact fetal RRI and HRV.

It is unknown when the similarities between maternal and fetal RRI tachograms arise and a solid answer for this requires developing devices that can measure fHR when it starts beating. However, rough speculations regarding the inception of similarities between maternal and fetal RRI can be made from the knowledge in previous literature. Fetal heart formation starts at around the third week and then starts beating by the fourth week (55). Previous literature indicated that the average fHR is around 110 beats per minute (bpm) around the 5^{th} week (55). After the 5^{th} week, the average HR increases until the 11^{th}-12^{th} week and then decreases again near term (55). Concerning mHR, it was found to increase with GA from around the 10^{th} week (56) and this coincides with the decrease in fHR after the 11^{th} – 12^{th} week. Hence, we speculate that the similarities arise as early as the 10^{th} week.

It is worth mentioning that our conclusions regarding the increase in similarity with GA, Table 1, were based on 5-minute segments, hence, analysis of different time segments may provide different results. Also, different results could be obtained if different methods were for similarity assessments. We collected our data in a supine position which is known to reduce HR (57,58), hence it is unknown how similarities along with their assessments would change with body postures.

3.7 Limitations and Conclusion

In this chapter, the concept of similarities between maternal and fetal RRI tachograms was discussed. The similarities were mathematically quantified by using CC analysis. Correlation analysis between CC coefficients and GA revealed that the similarities are associated with fetal development. Further, a comparison of means analysis revealed that similarities affect maternal and fetal HRV and they are specifically associated with mVLF.

The retrospective design of the study constitutes the major limitation. Our sample consisted of subjects of different ages and pregnancy complications, which might have affected the correlations to some extent. We did not consider the time lag between maternal and fetal RRI tachograms which could have enriched our conclusions. Further, fetal behavioral states (38) and fetal gender (59,60) are known to affect fetal HRV, therefore, they might have also affected the correlations as well. However, effects related to pregnancy complications, age, or fetal behavior do not alter the major finding of our study, the presence of similarities and associations between maternal and fetal HRs and HRVs.

Chapter 4: Pattern-based maternal-fetal HRV correlation

4.1 Brief overview of the chapter

In chapter 3, similarities between maternal and fetal RRI tachograms which can be, sometimes, visually observed were discussed. Similarities were quantified by using CC and they were found to be associated with fetal development. Also, mVLF was found to be associated with the similarities. Therefore, in this chapter, the association between mVLF and fetal development is investigated by means of correlation analysis between fetal HRV and mVLF. The presence of similarities between maternal and fetal HRV suggests the need to develop biomarkers that depend on both HRV parameters to assess pregnancy outcomes and fetal development. In this chapter, an HRV parameter that was derived from both maternal and fetal HRV is discussed. The parameter was calculated from the number of R peaks per 2 seconds (nRpp2s). The association between the parameter and fetal development was investigated and it was further used to divide data into three patterns to investigate the correlations between maternal and fetal HRV. Figure 5 provides a summary of this chapter.

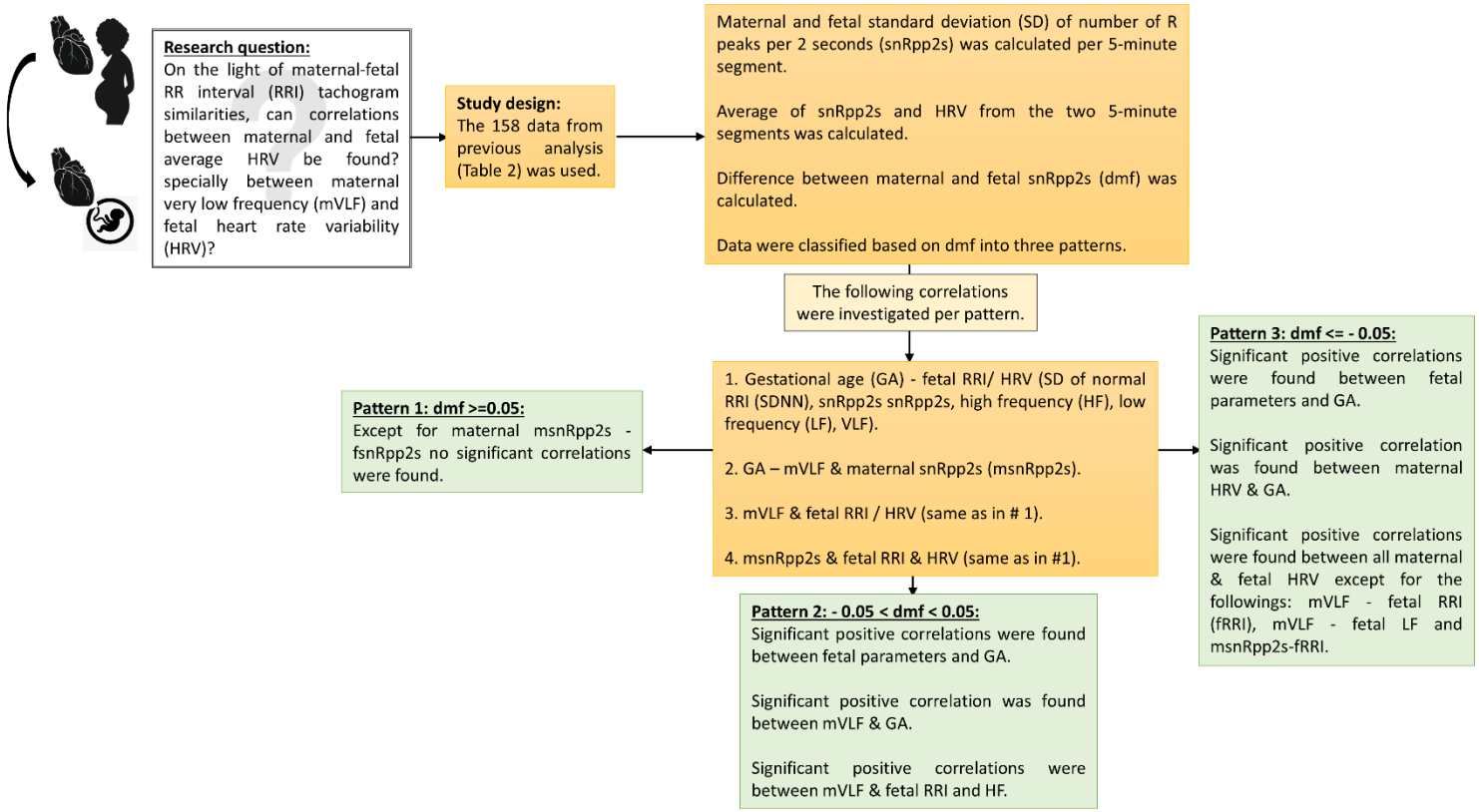

Figure 5: Illustrative summary of chapter 4

4.2 Methods

4.2.1 Data selection and analysis

Methods regarding data analysis and selection are similar to what has been discussed in sections 3.2.1 and 3.2.2. In this chapter, data from the 158 subjects in which extraction of 2 segments of 5-min was possible is used (Table 2). HRV analysis was discussed in section 3.4. After calculating HRV per 5-min segment, the average was taken for the analysis in this chapter.

4.2.2 nRpp2s calculation

nRpp2s analysis was performed in MATLAB. A code was developed to count the number of R peaks occurring within a 2-second window. After that, the SD of nRpp2s (snRpp2s) was calculated to calculate the difference between maternal and fetal snRpp2s (dmf). dmf was calculated by subtracting fetal nRpp2s (fsnRp2s) from maternal nRpp2s (mnRpp2s) (mnRpp2s – fnRpp2s) with considering 4-digit numbers. Patterns were classified based on dmf as follows: pattern 1: dmf >= 0.05, pattern 2: - 0.05 < dmf < 0.05 and pattern 3: dmf <= - 0.05.

4.2.3 Statistical analysis

Normality tests were conducted in MALTAB by using the One sample Kolmogorov-Smirnov test (kstest) and the Shapiro-Wilk test (swtest) (35). Kstest results showed that all variables were non-normally distributed regardless of the pattern but swtest showed discrepancies among the patterns. Therefore, normality tests were based on kstest only. Correlation analysis between two variables was performed by using the spearman test.

4.3 Demonstration of nRpp2s

The upper panels of Figure 6 show maternal (blue) and fetal (red) RRI tachograms, and the lower panels of Figure 6 show examples of nRpp2s plots. In Figure 6A (lower panel), the mnRpp2s changed more than that of the fetus. In Figure 6B, the rate of change of maternal and fetal nRpp2s was roughly the same, and in Figure 6C (lower panel), the rate of change in fnRpp2s was higher than that of the mother. The rate of change was quantified by using snRpp2s.

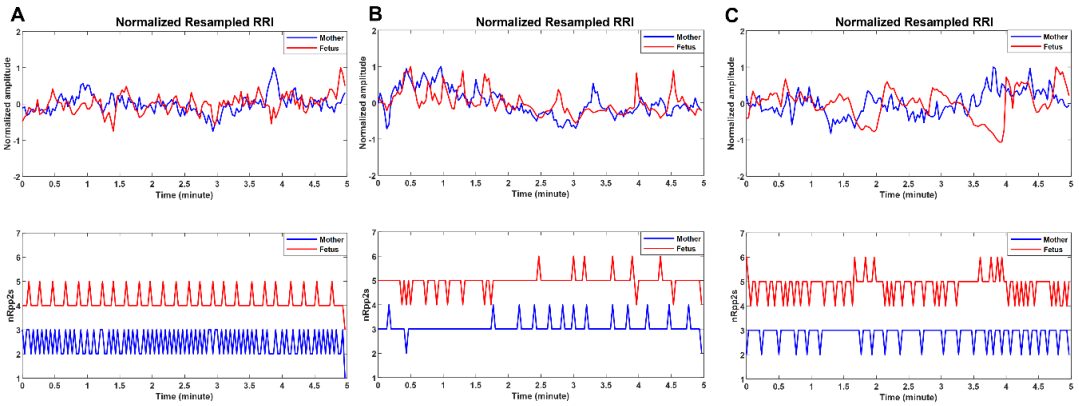

Figure 6: Demonstration of the number of R peaks per 2 seconds (nRpp2s): The upper panels show maternal (blue) and fetal (red) RR interval (RRI). The lower panels show the maternal and fetal number of R peaks per 2 seconds (nRpp2s). (A) The rate of change in mnRpp2s (blue) is higher than fnRpp2s (red), fetal standard deviation of nRpp2s (fsnRpp2s): 0.39, maternal snRpp2s (msnRpp2s): 0.51, GA: 37 weeks. The figure is an example of pattern 1. (B) The rate of change in maternal and fetal nRpp2s is roughly similar, fsnRpp2s: 0.35 msnRpp2s: 0.309, GA: 23 weeks, pattern 2. (C) Opposite to (A), the rate of change in fnRpp2s: 0.50 is higher than mnRpp2s: 0.37, GA: 29 weeks, pattern 3.

4.4 Difference between maternal and fetal snRpp2s (dmf)

Figure 7A shows the distribution of snRpp2s relative to RRI. The figure reveals a parabolic distribution in both maternal (blue) and fetal (red) snRpp2s. Compared to fsnRpp2s distribution, msnRpp2s distribution is larger which is expected due to the more developed maternal cardiac system. The difference between maternal and fetal snRRp2s was found to significantly decrease with GA in Figure 7B. Figure 7B shows that pattern 3 occurs more often at advanced GA whereas, pattern 1 occurs at earlier GA.

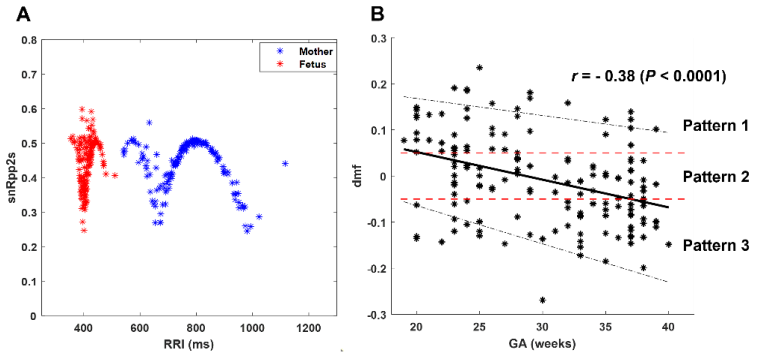

Figure 7: Demonstration of the maternal and fetal standard deviation of the number of R peaks per 2 seconds (snRpp2s) and their difference (dmf). (A) maternal (blue) and fetal (orange) snRpp2s show parabolic distribution with RR interval (RRI) and the difference between them (dmf) in (B) decreases with gestational age (GA), *r* is the spearman correlation coefficient. The red dotted lines in (B) show the threshold values, - 0.05 and 0.05, that were used to divide the data into three patterns, pattern 1: dmf >= 0.05, pattern 2: 0.05 < dmf < - 0.05 and pattern 3: dmf <= - 0.05. The black dotted lines show the 95% confidence interval of regression between the dmf and GA.

4.5 Correlation between maternal and fetal HRV per pattern

Table 4 shows the results of the correlation between maternal and fetal HRV, additionally, the correlations between each of the latter and GA are also provided. Among the three patterns, pattern 3 has the highest incidence of significant correlations between maternal and fetal HRV, and between GA and HRV. In pattern 3, mVLF was found to be correlated with all fetal parameters except LF and RRI. Further, msnRpp2s was significantly correlated with all fetal parameters except RRI. Both maternal snRpp2s and VLF were significantly correlated with GA. With respect to fetal parameters, all of them were found to be significantly correlated with GA.

Table 4: Correlation between maternal and fetal HRV per pattern

Pattern	Fetal Features	mVLF	msnRpp2s	GA
Pattern 1 n = 46	**RRI**	0.12	0.033	0.28
	snRpp2s	0.025	0.29*	- 0.10
	SDNN	0.01	0.23	- 0.04
	HF	0.031	0.20	0.11
	LF	- 0.13	0.062	0.17
	VLF	0.052	0.17	- 0.22
	GA	0.043	0.047	
Pattern 2 n = 54	**RRI**	0.35†	0.14	0.29*
	snRpp2s	0.062	0.76†	0.024
	SDNN	0.27	0.13	0.41†
	HF	0.36†	0.14	0.51†
	LF	0.20	0.17	0.32*
	VLF	0.24	0.18	0.38†
	GA	0.40†	- 0.035	
Pattern 3 n = 58	**RRI**	0.21	0.16	0.39†
	snRpp2s	0.45†	0.79†	0.69†
	SDNN	0.29*	0.63†	0.59†
	HF	0.26*	0.33*	0.54†
	LF	0.22	0.50†	0.46†
	VLF	0.31†	0.61†	0.56†
	GA	0.44†	0.57†	

*** P < 0.05, † P <0.005, HRV: heart rate (HR) variability, GA: gestational age, RRI: RR interval, SD: standard deviation, SDNN: SD of normal RRI, VLF: very low-frequency power, LF: low-frequency power, HF: high-frequency power. The values in the table indicate the spearman correlation coefficient (*r*).**

In pattern 2, except for snRpp2s, all fetal parameters were found to significantly increase with GA. In pattern 2, only mVLF was found to correlate significantly with GA. Compared to pattern 3, pattern 2 has less incidence of significant correlations between maternal and fetal HRV. In pattern 2, mVLF is significantly correlated with fetal RRI, and HF, also, in the same pattern, msnRpp2s is significantly correlated with fsnRpp2. Except for the fsnRpp2s-msnRpp2s correlation, there were no significant correlations in pattern 1. It is worth mentioning that the values of *r* were found to decrease from pattern 3 to pattern 1.

4.6 Discussion and physiological implications

In this chapter, the dmf factor, which was derived from maternal and fetal HRV (Figure 7B), was discussed. The factor was used to divide data into three patterns to explore the association between maternal and fetal HRV (Table 4). In addition, associations between HRV and GA were investigated per pattern. Correlation analysis revealed that pattern 3 had major information regarding fetal development. Also, pattern 3 had the highest incidence of significant correlations between maternal and fetal HRV and all of them were positive. The positive correlations are consistent with what has been reported in previous studies (24,25,15). *Leeuwen et al.* (24) showed that maternal and fetal SDNN were higher in pregnant women (GA = 36 weeks) who exercised compared to the control group. *L. Igor* (25) found that both maternal and fetal HRV (including SDNN and VLF) were decreased in pregnant women who had mild and severe pre-eclampsia compared to the control group, GA= 34 - 40 weeks. *H. Haliza et al.* (15) found that fetal SDNN of obese or overweight pregnant women was reduced. Obesity was associated with reduced HRV (61,62), hence, the reduction in fetal SDNN could have accompanied the reduction in maternal SDNN due to obesity. All the previous studies confirm the positive correlations we found between maternal and fetal HRV.

Table 4 shows there were discrepancies in *r* values among the patterns and based on such variations we speculate two implications. The first one could be related to the maternal-fetal RRI tachograms similarities. In chapter 3, we addressed that the similarities occur due to a regulation that mediates both. Given the latter, it could be that the impact of the regulation is lowest in pattern 1. And according to the results, it can be implied that such regulation had a major role in fetal HRV and ANS development. The second implication could be based on the development of fetal behavioral states and ANS activity. The incidence of pattern 3 increases with GA which coincides with fetal development as well. But the second implication does not justify the absence of correlations between maternal HRV and GA since maternal HRV is well-developed compared to the fetus. Hence, the variations among the patterns can be more justified by the presence of physiological processes or regulations that mediate both.

Pattern 2 which is a transition state from early to advanced GA, had significant correlations between mVLF and GA and between fetal HRV and GA. However, the *r* values were lower than that of pattern 3. Based on Table 4, it can be concluded that patterns 2 and 3 hold more value for fetal development assessment based on HRV or HR collected from 5-min epochs. Moreover, pattern 3 holds more value in terms of the evaluation of the maternal impact on fetal development. It is worth mentioning that there were fewer correlations between maternal HRV and fetal RRI which was expected due to the

presence of negative and positive similarity trends. Therefore, the association between maternal HRV with fetal RRI, over the short term, could be more clarified by addressing negative and positive similarity trends. We could not perform such analysis due to the limited number of subjects.

The discrepancies found between the three patterns may justify the inconsistencies related to maternal-fetal HR coupling that was discussed in the introduction. Pattern-based analysis can provide a better understanding of how HRV may react to different stimuli such as respiration and exercise. Previously, it was addressed that HRV can be used to assess cardiovascular-related risks (63,64,65). For example, Hidase et al. (65) found that the VLF band was a strong predictor for cognitive heart failure (65). Therefore, understanding how fetal HRV changes relative to maternal HRV may provide a better understanding of cardiovascular complications that occur in both the mother (post-pregnancy) and the fetus (after birth). So far, little knowledge is available regarding the norm behind the correlations between maternal and fetal HRV, and more research is needed to clarify this for a better assessment of fetal health.

Remarks on choosing 2 seconds for the analysis in chapters 3 and 4

A 2 seconds window size was chosen for two main reasons. The first involve the maternal RRI range. The maximum average maternal RRI value was 1125 ms, hence, we attempted at choosing the lowest possible window size to capture detailed beat-by-beat variations induced simultaneously by fetal and maternal HRV. The second reason involve the results related to the correlation between dmf and GA. We attempted calculating dmf for 1.5 and 3 seconds and the correlations with GA were 0.0787($P > 0.05$) and 0.079 ($P > 0.05$), respectively. Since the correlations for 1.5 and 3 seconds were insignificant we based our analysis on two seconds.

4.7 Limitations and Conclusion

In this chapter, an HRV factor based on maternal and fetal HRV was discussed. The factor was found to be related to fetal development and it was used to divide data into patterns. Correlation analysis between maternal and fetal HRV per pattern revelated positive significant correlations exist between both HRV. The findings highlight the importance of maternal condition on the fetal cardiovascular system and development. The limitations of the study discussed in this chapter are similar to what has been discussed in chapter 3.

Chapter 5: Artificial intelligence-based model for fRRI prediction

5.1 Brief overview of the chapter

Given the associations that were found between maternal and fetal HR/HRV in chapters 3 and 4, we investigated the possibility of developing an AI model to predict fRRI from maternal factors in this chapter. Recently, many AI techniques have proven useful in medical applications and the scope of their application is considered limitless (66), for example, they have been used for the identification of important features to build predictive models for heart failure (67) and systolic heart failure survival rate (68). Developing AI models could assist physicians in the diagnosis process which can save them time.

In this study, we used two supervised learning techniques, support vector regression (SVR) and random forest (RF) to predict fRRI from maternal factors. Based on the available data in our study, we identified features that we speculated to be useful for fRRI prediction. Oxygen and nutrition delivery to the fetus is dependent on maternal respiration and blood circulation, therefore, we opted for choosing variables that are related to them which included RRI, HRV, R wave amplitude variability (RWAV), age, and weight. RRI was included in the model based on the previously mentioned correlations between maternal and fetal HRs. HRV, which is an indicator of ANS (30,36) activity, was found to change due to respiration (36). Further, RWAV was associated with respiration and stroke volume (69,70). Age (71) and weight (72) were included in the model because they were found to be associated with HRV. Figure 8 provides a summary of chapter 5.

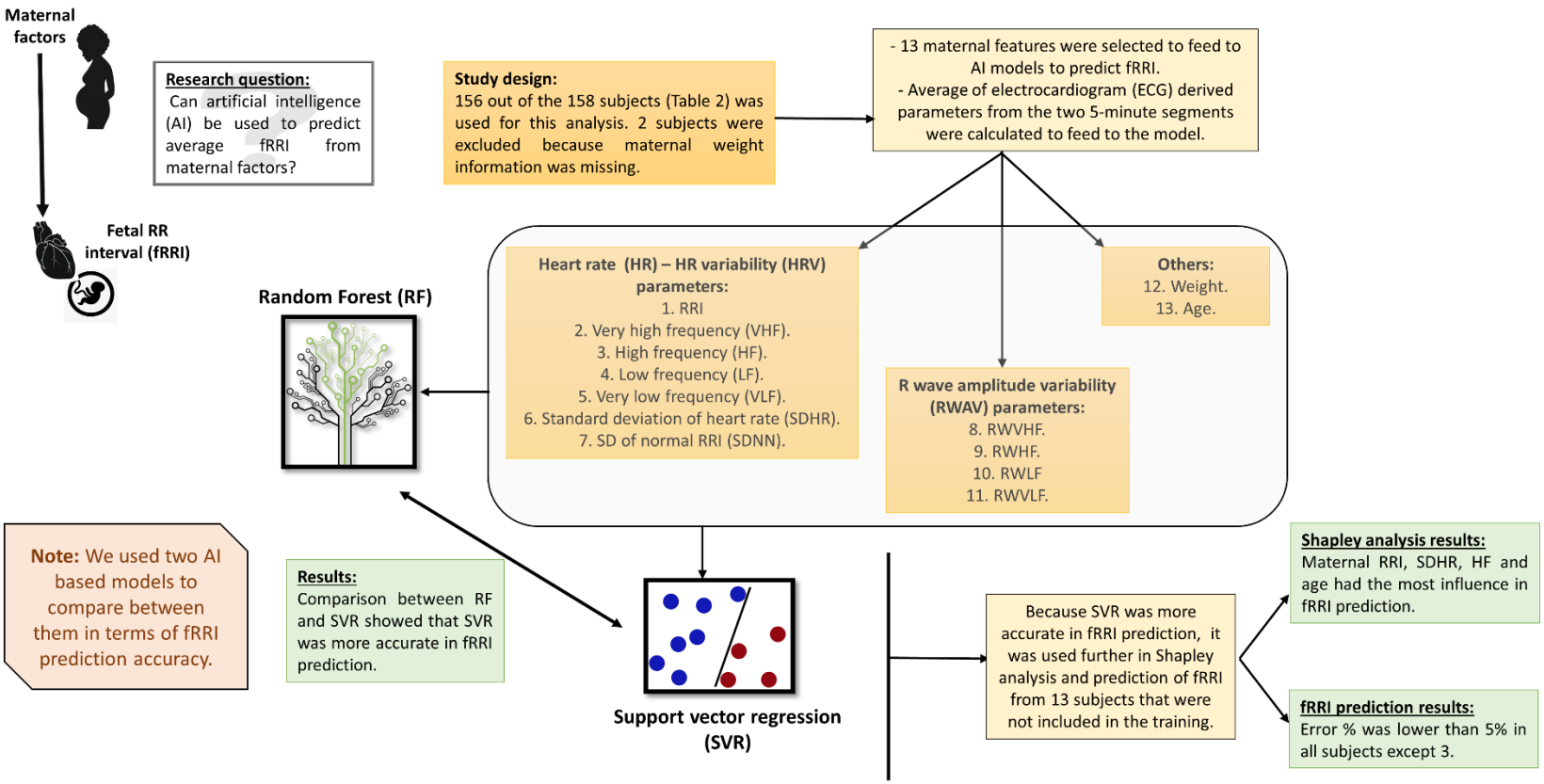

Figure 8: *Illustrative summary of chapter 5*

5.2 Methods

5.2.1 Data Selection

The data used here included the same subjects discussed in chapters 3 and 4. From the 172 subjects, we used data from the 158 subjects in which extractions of two segments of 5-min were possible (Table 2). From the 158 subjects, data from 156 subjects were used for training the model; 2 subjects were not used because information regarding maternal weight was missing. For further validation of the model, data from the remaining 14 subjects (with one segment of 5-min) was used to predict fRRI values.

5.2.2 Heart rate variability (HRV) and R wave amplitude variability (RWAV) analysis

The methods followed for HRV analysis were the same as what has been discussed in section 3.4, however, the very high frequency (VHF) band has been added here with the following range (73): (0.4 - 0.9) Hz. Compared to HRV analysis, there is less literature concerning RWAV. In our study, we calculated RWAs by normalizing the RWA values. Then, a new signal was obtained from the variations exhibited in RWA values. The normalized RWA values were used to calculate frequency-based RWAV by using the same frequency bands, VLF, LF, HF, and VHF. To distinguish HRV features from that of RWAV, the term RW will be used to refer to RWAV features (RWVLF, RWLF, RWHF, RWVHF).

5.2.3 Machine learning models and Shapley analysis

MATLAB 2022a was used for developing the models and Shapley analysis. Two regression machine learning techniques were used for the prediction of average fRRI which are SVR and RF. SVR, which is an expansion from SV machine (SVM), is a non-parametric supervised learning algorithm that relies on kernel functions to optimize models by finding the best-fit lines with hyperplanes (74). In MATLAB, SVR utilizes the linear epsilon insensitive (ε) SVM regression to find a function *f(x)* that does not deviate from response values by more than ε (75). RF is a supervised learning algorithm. RF is an ensemble technique that optimizes models based on many aggregated bootstrap decision trees (76). For cross-validation, we used leave-one-out in which one data is used for testing and the rest is used for training.

Since SVR and RF are supervised learning algorithms, features should be fed to models for training and testing. In our study, features that were fed to the models were calculated out of the extracted 5-min segments. As was described before, two segments of 5-min were obtained from 156 subjects and the average of features per subject was fed to the models. The total number of maternal features that were fed to the models was 13 which included: 1. Age, 2. Weight, 3. SDNN, 4. SDHR, 5. VLF, 6. LF, 7. HF, 8. VHF,

9. RWVLF, 10. RWLF, 11. RWHF, 12. RWVHF, 13. RRI. Figure 9 shows a summary of the steps that were followed for data analysis.

To get an interpretation of the model, we applied Shapley analysis. Shapley analysis is stemmed from game theory and basically, it calculates the contribution of a feature to predicting values (77,78). In other words, Shapley's values can provide a general idea about the importance of a feature. Shapley values can be negative or positive and here we considered positive values only because we were interested in the absolute value regardless of the sign. Shapley values were calculated by taking the absolute average from the 156 subjects.

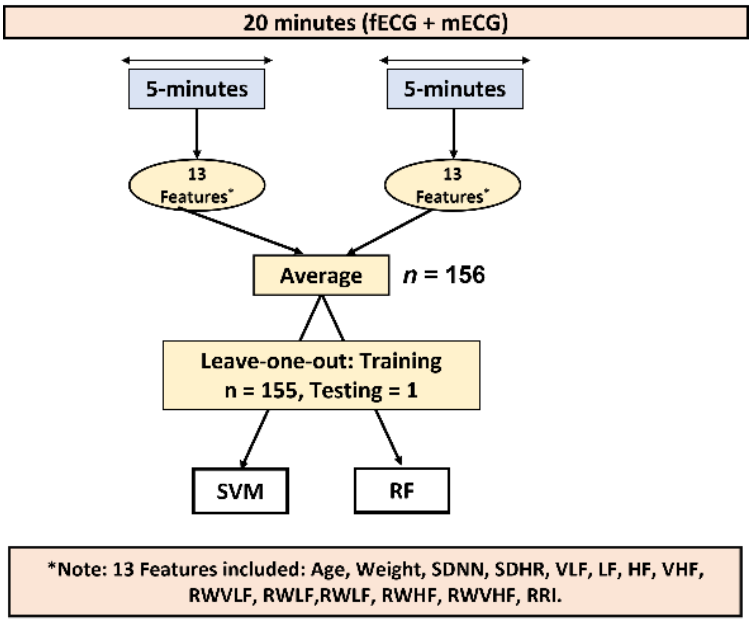

Figure 9: Summary of data analysis. Following extraction of maternal and fetal electrocardiogram (ECG), 13 features were calculated per 5-minute segments. The average from the two 5-minute segments was then fed to two models, support vector regression (SVR) and random forest (RF).

5.2.4 Model evaluation

To evaluate model performance, Bland-Altman (BA) (79,80) and spearman correlation analyses were performed to compare the predicted and model-based values. Also, root mean square error (RMSE) and error percentages were calculated. The developed model was also tested on the 14 subjects that were not used in the training.

5.3 Results

5.3.1 Summary of the features

Table 5 shows the mean and SD values for the maternal features and fRRI. The first 13 features in the table were fed to the SVM and RF models to predict the 14th feature, fRRI.

Table 5: Mean and SD values of maternal features and fRRI

Feature	(mean ± SD)
RRI (ms)	763 ± 114
SDNN (ms)	34 ± 14
SDHR (bpm)	3.6 ± 1.3
VHF (ms^2/Hz)	44 ± 146
HF (ms^2/Hz)	254 ± 356
LF (ms^2/Hz)	229 ± 223
VLF (ms^2/Hz)	664 ± 565
RWVHF (ms^2/Hz)	0.016 ± 0.012
RWHF (ms^2/Hz)	0.056 ± 0.040
RWLF (ms^2/Hz)	0.019 ± 0.011
RWVLF (ms^2/Hz)	0.037 ± 0.025
Age (years)	34 ± 5.3
Weight (Kg)	60 ± 8.4
fRRI (ms)	412 ± 24

SD: standard deviation. RRI: RR interval, SDNN: SD of normal RRI, SDHR: SD of heart rate. bpm: beats per minute. VHF: very high frequency, HF: high frequency, LF: Low frequency. VLF: very low frequency. RWVHF: R wave very high frequency, RWHF: R wave high frequency, RWLF: R wave low frequency, RWVLF: R wave very low frequency. fRRI: fetal RRI.

5.3.2 Comparison between SVR and RF performance

Figure 10 shows plots of error percentages versus GA which show that error percentages did not change with GA in both models. Figure 11 shows the results of correlation and BA analyses for the SVR (Figure 11 A-B) and RF (Figure 11C-D) models. In Figure 11, it is revealed that the SVR model has higher accuracy compared to the RF model due to its lower RMSE and error values. Also, the value of the correlation coefficient (*r*) for the SVR model (Figure 11A) is higher than that of the RF model (Figure 11 C). In BA plots (Figure 11B and Figure 11D), the percentage of points that were within the limits of agreement was around 95%, nevertheless, the boundaries in (B) were narrower than (D) implying higher accuracy for the SVR model. In BA plots, it is shown that both models generally underestimate the predicted values and according to the mean values, it is revealed that SVR has higher accuracy due to the lower mean value compared to the RF model. Due to the higher accuracy of the SVR model, it was used further for Shapley analysis and prediction of fRRI values that were not involved in the training.

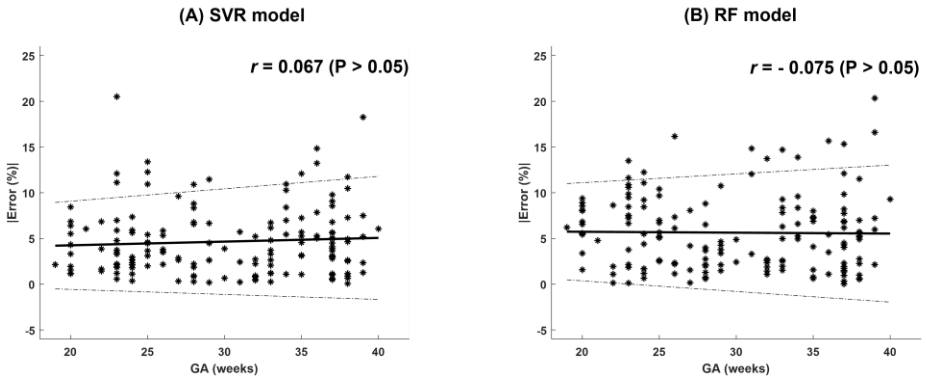

Figure 10: Absolute error percentage versus gestational age (GA). (A) support vector regression (SVR) model. (B) Random forest (RF) model.

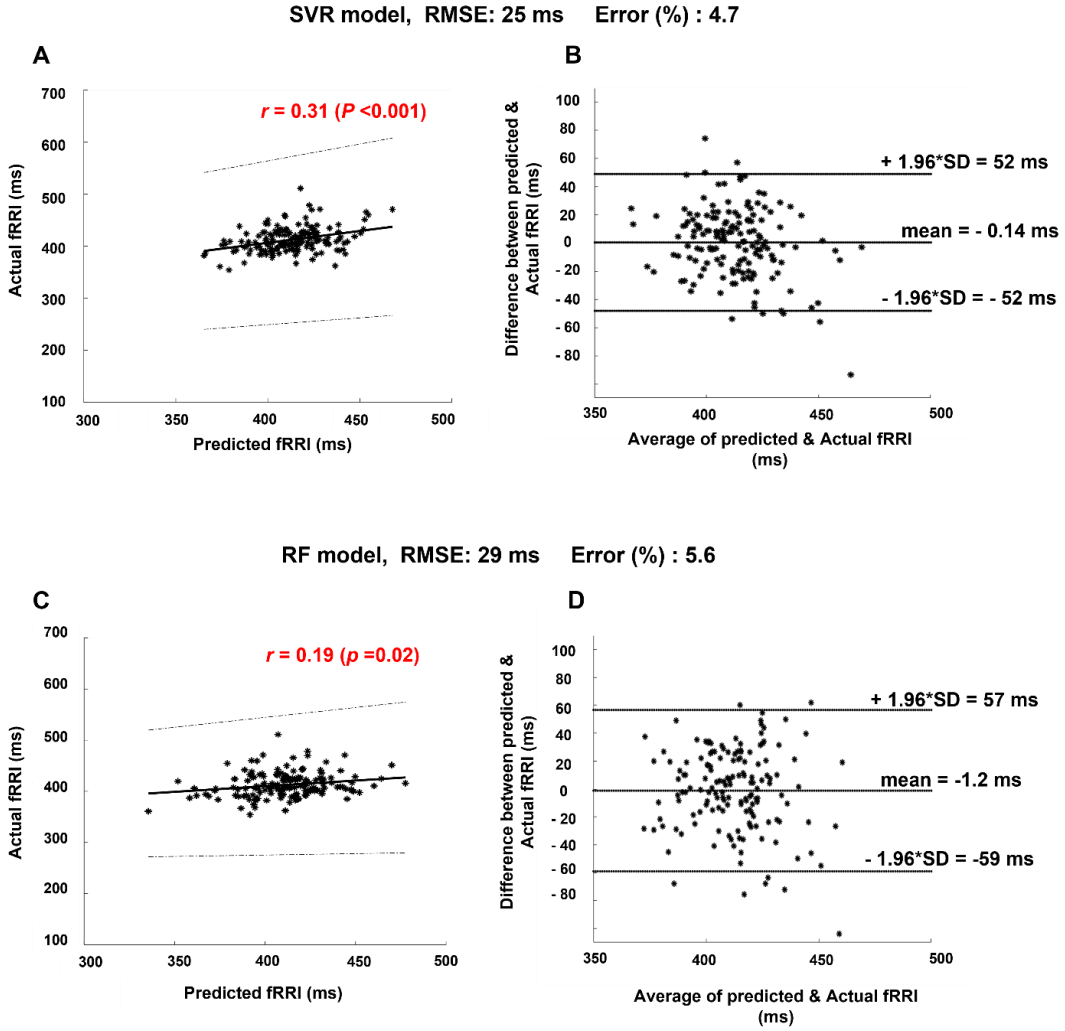

Figure 11: Bland Altman (BA) and correlation analysis. (A) shows the results of the support vector machine (SVR) model and (B) shows the same for the random forest (RF) model. The limits of agreement of BA plot, root mean square error (RMSE), and error percentage are lower in the SVR model. Also, the spearman correlation coefficient (*r*) value of the SVR model is higher than that of the RF model. The latter facts show that the SVR model was more effective in the prediction of fRRI values.

5.3.3 Shapley analysis

The absolute average values of Shapley along with the 95% confidence interval are shown in Figure 12. In the figure, it is revealed that among the 13 features, age, HF, SDHR, and RRI had a major effect on fRRI predictions whereas VHF was found to have the lowest impact.

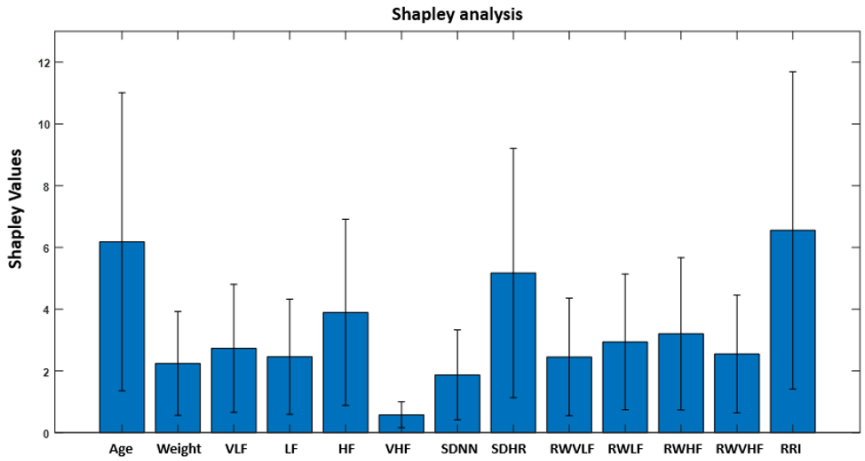

Figure 12: Average Shapley values with 95% confidence interval (CI): Shapley analysis shows that age, HF, SDHR, and RRI had the highest impact on average fetal RR interval (fRRI) prediction whereas very high frequency (VHF) had the lowest impact.

Table 6: SVR model prediction of fRRIs.

Subject number (GA (weeks))	Maternal age (years)	Maternal complication	Actual fRRI (ms)	Predicted fRRI (ms)	Error (%)
1 (28)	43	Uterine / appendix disease	445	434	2.5
2 (32)	43	Uterine / appendix disease	434	420	3.3
3 (37)	30	Uterine / appendix disease	412	416	0.9
4 (25)	**39**	Uterine / appendix disease	**408**	**435**	**6.5**
5 (29)	**35**	Uterine / appendix disease	**385**	**438**	**14**
6 (37)	31	Central nervous system disease (CNS)	370	388	4.9
7 (23)	29	None	419	418	0.4
8 (26)	30	None	383	370	3.0
9 (29)	29	Autoimmune disease	432	422	2.2
10 (37)	42	CNS, Bone muscle diseases, Multiple sclerosis	446	431	3.1
11 (38)	27	Mental illness	409	429	5.0
12 (38)	32	Mental illness	407	420	3.1
13 (39)	**45**	**Respiratory disease, uterine/appendix disease**	**502**	**410**	**18**
14 (33)	32	Psoriasis vulgaris	418	435	4.1

5.3.4 Model validation on test subjects

After developing the model, we attempted to predict fRRI values from the 14 subjects that were not considered in training the model. The results of prediction per subject are listed in Table 6. Error percentages were calculated to estimate the accuracy of prediction and as the table shows, they were less than or equal to 5 % in general except in 3 cases (subjects # 4, 5 &13).

5.4 Discussion

In this study, we investigated the possibility of predicting average fRRI values from maternal factors by using SVR and RF models, we used both HRV and RWAV along with weight and age for the prediction of fRRI. We speculated that the dynamics exhibited in mRRI or RW can potentially be used for the prediction of fRRI. We used time and frequency-based HRV parameters for the prediction. With respect to RWAV, we used frequency-based parameters only because we were more interested in RWAV which are known to be affected by respiration (69,70). Because it is unknown which and how maternal HR or RW -based factors affect fRRI we used the whole frequency power spectrum and we divided them into the four known bands (VLF, LF, HF, and VHF) to get more perspectives on which bands are more predictive of fRRI. Understanding the exact bands that contribute to fRRI prediction can give more insight on the connection between maternal ANS and respiration with fRRI. Due to the complex correlation between maternal factors and fRRI, we opted for using machine learning-based techniques for the prediction of fRRI.

We developed two models and a comparison analysis between SVR and RF models revealed that SVR outperformed RF in predicting fRRI (Figure 11). Due to the better performance of SVR, we used it further in Shapley analysis (Figure 12) and prediction of fRRI from the 14 subjects that were not used in the training (Table 6). In Figure 12, it is demonstrated that between age and weight, age had a stronger effect on fRRI prediction. Further, the figure shows that among the ECG-derived parameters, maternal RRI, SDNN, and HF had the highest impact on fRRI prediction.

As was mentioned in the introduction, the effect of maternal HR or RRI on fHR was document on previous studies (11,18,21). However, the association of maternal age, HF and SDHRs with fHR is less documented. In previous studies (81,82), it was addressed that advanced maternal age was associated with preterm delivery and small for gestational age (82), but the mechanisms related to this are not fully understood yet. In our study, we show that maternal age has a strong impact on fRRI (Figure 12), which could be one of the pathways by which maternal age affects fetal development. At advanced age, there is a tendency for HRV to decrease and for blood pressure to increase which may lead to health

complications without proper management (83). As a result, fRRI is expected to get affected by age-related changes in maternal cardiac functionality. The effect of maternal HRV on fRRI is still to be understood but previously it was demonstrated that maternal breathing affected maternal and fetal HR coupling (14). Respiration is known to affect HRV, especially the HF band (30,36), hence, the associations of fRRI with maternal SDHR and HR that were found in our study could be respiratory mediated, but more research is needed to validate this.

Table 6 shows that the model was generally effective in predicting fRRI since the error percentages were less than or equal to 5% except in three cases, subjects # 4, 5 & 13. We expected to find deviations between the actual and predicted values because we speculate that the maternal effect on fRRI is partial and not dominant because fRRI is controlled by many physiological processes such as fetal behavioral states (38). Also, we expect that maternal complications may affect the prediction's accuracy. It is worth mentioning that, due to the limited knowledge in the field, it is unknown if a particular measured fRRI value indicates a norm or not. Hence, training predictive models to distinguish a norm could assist physicians in the assessment of fetal health. Model-based prediction of fRRI from the maternal condition is yet to be explored and so far, it is unknown which machine-learning technique could be suitable for this type of application. Therefore, in this study, we opted for using two of the commonly used techniques for regression, SVR, and RF.

5.5 Limitations and conclusion

Although our results show that our SVR model was efficient enough and provided a high level of performance, it has several limitations. Our retrospective design constitutes a major limitation. As was mentioned in Methods (chapter 3), pregnant women had complications and we expect that such complications affected the accuracy of the model. Also, we expect that inclusion of more maternal-related information may enhance the model accuracy such as maternal blood pressure, respiratory rate, and height. Maternal height was not available for all subjects; hence, it was not included as a feature in our model.

In conclusion, we demonstrated that fRRI can be predicted from maternal factors by using machine learning-based models. The dependency between maternal and fetal RRI that was reported in this chapter suggests that fetal development and health assessment can be enhanced by integrating maternal conditions.

Chapter 6: Maternal-fetal RRI similarities in mice

6.1 Brief overview of the chapter

In chapter 3, similarities between maternal and fetal RRI tachograms in human subjects were discussed. The similarities were found to be associated with fetal development. In this chapter, a similar analysis to what has been covered in chapter 3 is discussed but with data from mice. In this chapter, four coefficients are discussed, the previously mentioned CC3 and CC4 along with two additional coefficients denoted as coherence low frequency (CLF) and coherence high frequency (CHF). In this chapter, CC3 and CC4 are referred to as CCm1 and CCm2, respectively. Similar to what has been reported in chapter 3, the coefficients were found to significantly change with embryonic days (EDs). After confirming the association between the similarity and fetal development in mice, we opted for investigating similarity trends in the ASD mouse model. The model was made by injecting the mother with valproic acid (VPA) on ED12.5 to make the treatment group. The control group was made by injection of saline on ED12.5. Comparison between the control and VPA mouse in terms of CC1m, CLF, and CHF revealed differences between both. Figure 13 provides an illustrative summary of the chapter.

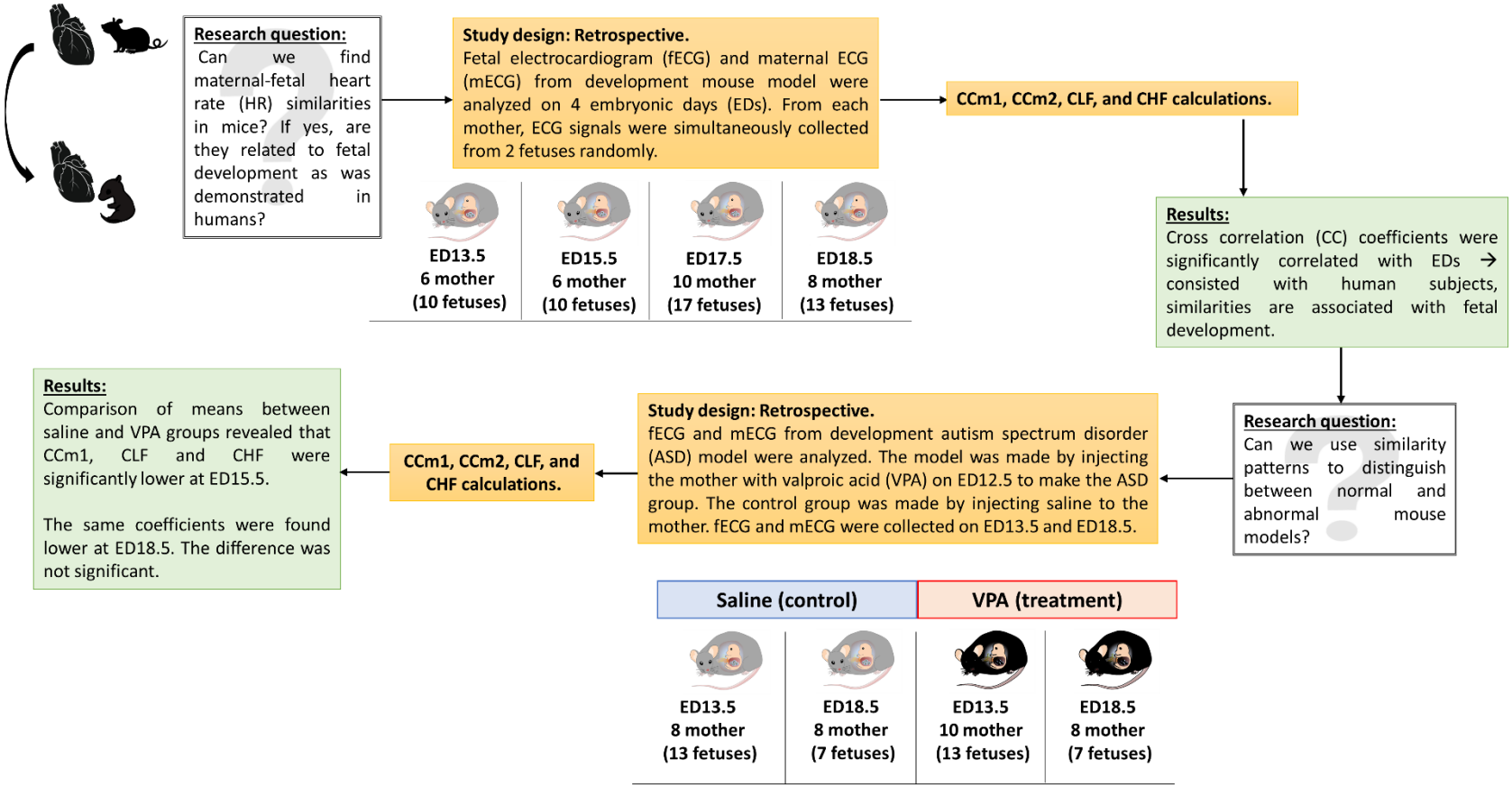

Figure 13: Illustrative summary of Chapter 6.

6.2 Method

6.2.1 Animal handling

The data used in this chapter were analyzed retrospectively and they were mentioned in our previous studies (84,85). Animal handling and experimental protocols were per the Guidelines for the Care of Laboratory Animals of Tohoku University Graduate School of Medicine. The protocols were approved by the Committee on Animal Experiments at Tohoku University, Sendai, Japan (study approval number: 2017MdA-334). Before mating, C57BL6/J female mice (CLEA, Tokyo, Japan) were housed socially in 3-5 groups in cages under control lightning of 12h:12h light-dark cycle. Mice had unlimited access to water and food. For mating, female mice (7-19 weeks of age) were housed in cages with male mice of similar age (1 male and 1 female mouse per cage) in the evening and then separated the next morning. To make the VPA model, 600 mg/kg of valproic acid sodium salt (VPA; Sigma, St. Louis, MO, USA) dissolved in saline solution was injected into the subcutaneous fat of the pregnant mother's neck on ED12.5. The control group of mice had only saline solution injected into them at the same location.

6.2.2 Experimental protocol

Before collection of ECG, pregnant mice were anesthetized with subcutaneous administration of ketamine (Ketalar 500 mg, 100 mg/kg; Daiichi-Sankyo, Tokyo, Japan) and xylazine (Rompun 2% w/v solution, 10 mg/kg; Bayer, Leverkusen, Germany) and maintained under anesthetic with inhalational isoflurane (0.5%, 260 ml/min; Forane AbbVie Inc., Chicago, IL, United States). The depth of anesthesia was assessed by using a toe pinch test. The combination of isoflurane with ketamine-xylazine was used to ensure the maintenance of stable anesthesia during ECG measurements. We could successfully use the same anesthetic combinations to measure clear and stable records of fECG in our previous studies (84,86). The ECG recording setup is explained in detail in our previous studies (84,86,23) .

The maternal mice were kept in a supine position and a far infrared heater was placed beside the maternal body to maintain a warm environment. Mice abdominal hair was removed using a hair removal cream (Veet, Reckitt Benckiser Group plc, Slough, England, UK). After confirming the mice were under anesthesia by the disappearance of movements, the abdomen was opened at the peritoneal cavity with fine scissors, and the uterus was exposed. The ECG was measured at a sampling rate of 1000 Hz for 15 minutes. mECG was recorded by attaching three electrodes to the maternal body. The configuration of ECG placement in mice is similar to that of Lead I, II, and III in humans where two leads are attached to the arms and one attached to the leg for grounding. fECG was recorded by attaching two electrodes, one at the fetal chest and the other at the back(the ground was the maternal body), fetuses were selected

randomly during recording. The ECG data were recorded by a portable multi-purpose bio signal amplifier monitoring system (Polymate AP1532 and AP Monitor; Miyuki Giken, Tokyo, Japan).

Fetal mouse development:

For fetal mouse development (85), simultaneous records of mECG and fECG of 2 random fetuses (from the same mother) were collected at embryonic days of ED13.5, ED15.5, ED17.5, and ED18.5. The total number of ECG data that were considered for analysis in this study was: ED13.5: 10 mothers (20 fetuses), ED15.5: 8 mothers (16 fetuses), ED17.5: 11 mothers (22 fetuses), ED18.5: 12 mothers (24 fetuses).

ASD mouse model:

For the ASD mouse model (84), simultaneous records of mECG and fECG of 2 random fetuses (from the same mother) were collected on ED15.5 and ED 18.5. The total number of ECG records that were considered for this study was: E15.5: Saline: 8 mothers (16 fetuses), VPA: 8 mothers (16 fetuses). E18.5: Saline: 8 mothers (16 fetuses), VPA: 7 mothers (14 fetuses).

6.2.3 Data analysis

All analysis was conducted in MATLAB 2022a. The first-minute segments of ECG records were excluded from the analysis due to noise. ECG records were examined to find two segments of 3-minute epochs with no noise or consistent arrhythmia. In all mice, except for 3 cases, the 3-min epochs were chosen consecutively. The two 3-min epochs were chosen from the 14 minutes of ECG recordings regardless of order (beginning, middle, or end of the recording). Data that did not have at least two 3-minute epochs of clear ECG recordings were excluded from the study. Hence, the total number of data that was included in the analysis is summarized in Table 7. A window size of 3-min was used for analysis because it was the maximum window size that could be considered with no arrhythmia or noise in the middle in all subjects.

Table 7: Summary of sample size

Mouse Group	ED13.5	ED15.5	ED17.5	ED18.5
Development	6 mothers (10 fetuses)	6 mothers (10 fetuses)	10 mothers (17 fetuses)	7 mothers (11 fetuses)
ASD		**Saline:** 8 mothers (13 fetuses)		**Saline:** 5 mothers (7 fetuses)
		VPA: 8 mothers (13 fetuses)		**VPA:** 5 mothers (7 fetuses)

ED: embryonic day, ASD: autism spectrum disorder, VPA: valproic acid

6.2.4 Measuring similarities between maternal and fetal RRI tachograms

Maternal and fetal RRI tachograms were resampled at 2 seconds by taking the average of RRI per 2 seconds to unify the lengths of both signals. A minimum of 2 seconds was used to accommodate for fRRI (the maximum average fRRI was around 928 ms). After that, the resampled signals were normalized by subtraction of mean values and then division by maximum values. After normalization, similarities were measured by using "xcorr" (for CC analysis) and "mscohere" (for magnitude-squared coherence (MSC) analysis) functions MATLAB2022a. "xcorr" was used for time-based similarity estimation and "mscohere" was used for frequency-based similarity estimation. The codes that were used for similarity estimation are found in Appendix E.

To calculate similarity by using "xcorr", the resampled normalized signal was divided into 10 samples. After that, CC coefficients were calculated using the "normalized" option in MATLAB per 10 samples. The latter calculation yields a total of 9 CC coefficients per 3 minutes (180000/2000 = 90 samples). To obtain an overall CC score or coefficient for the whole 3-min epoch, the average of the 9 CC coefficients was calculated. With this approach, two similarity scores were obtained, CCm1 and CCm2. CCm1 was calculated by taking the absolute average whereas CCm2 was calculated by taking the average with considering signs.

The methods that were adopted for similarity estimation by using "mscohere" were similar to that of frequency HRV estimation in which the power spectrum is divided into bands. Here, we divided the power spectrum into two bands: LF and HF. The maximum frequency obtained from the "mscohere" is 0.25 Hz, so we used the following divisions: LF: [0.04 – 0.15] Hz, HF: [0.15 - 0.25] Hz. Since up until now, there are no well-defined bands for fetal mice to measure ANS activity, we used bands defined for humans (36) because the range of average fRRI in our experiment was [306 - 981] ms. Similarity estimation by "mscohere" was done by setting the window size to 10 and the sampling frequency to 0.5 Hz. After that, the power spectrum density was estimated per band. Similarity for the LF and HF bands will be denoted as coherence LF "CLF" & coherence HF "CHF", respectively. Figure 14 provides a summary of ECG and similarity analysis.

6.2.5 Statistical analysis

Before performing statistical analysis, normality tests were conducted in MATLAB2022a by using the Shapiro-Wilk test (swtest) (35). For normally distributed data, correlation coefficients were calculated by Pearson correlation analysis, otherwise, Spearman was used. Comparison of means analysis was

performed with one-way ANOVA for normally distributed data and with Wilcoxon test for non-normally distributed data.

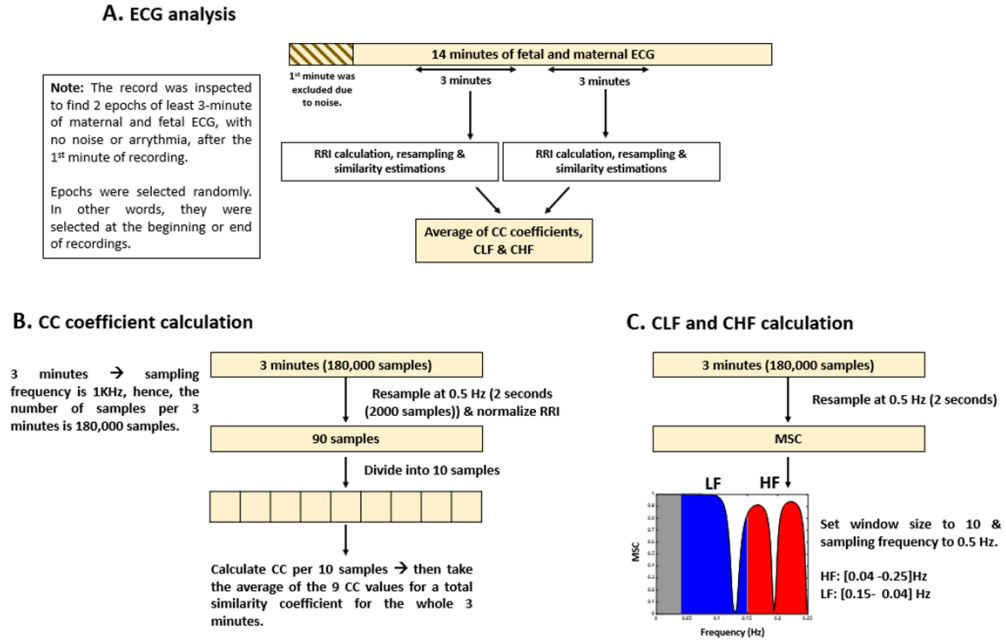

Figure 14: Summary of electrocardiogram (ECG) analysis and similarity estimations. The figure provides (A) an illustrative summary of the protocols that were followed to analyze ECG data, (B) calculation of cross correlation (CC) coefficients, and (C) coherence low frequency (CLF) and coherence high frequency (CHF) calculations.

6.3 Results

6.3.1 Fetal mouse development

- Demonstration of similarity patterns between maternal and fetal RRI tachograms in mice

Figure 15A, B, C, and D (A-D) show plots of normalized maternal (blue) and fetal (red) RRI tachograms from different developmental stages. Figure 15A and B (A-B) show examples of a positive similarity trend whereas Figure 15C and D (C-D) show examples of a negative similarity trend. In positive similarity trends, maternal and fetal RRI change in the same direction whereas in negative similarity trends, the same change in opposing directions. The upper panels of Figure 15C-D show the original changes in RRI and the lower panels show the same mRRI and the inversed fRRI tachogram to clarify the negative similarity trend. It is noticeable in Figure 15A-D that the degree of similarity between maternal and fetal RRI tachograms is more obvious at late developmental stages (ED17.5 and ED18.5).

Figure 16 shows an example of 2 fetuses from ED17.5 which belonged to the same mother with different similarity trends. In all three panels (top, middle, bottom), mRRI is the same. The top panel shows a positive similarity trend for fetus 1. The middle and bottom panels show RRI tachograms that belonged to the second fetus. In the bottom panel, fRRI is inversed to clarify the negative similarity trend. Figure 16 demonstrates that, at a given time, HRs of fetuses that belong to the same mother may correlate differently to maternal HR.

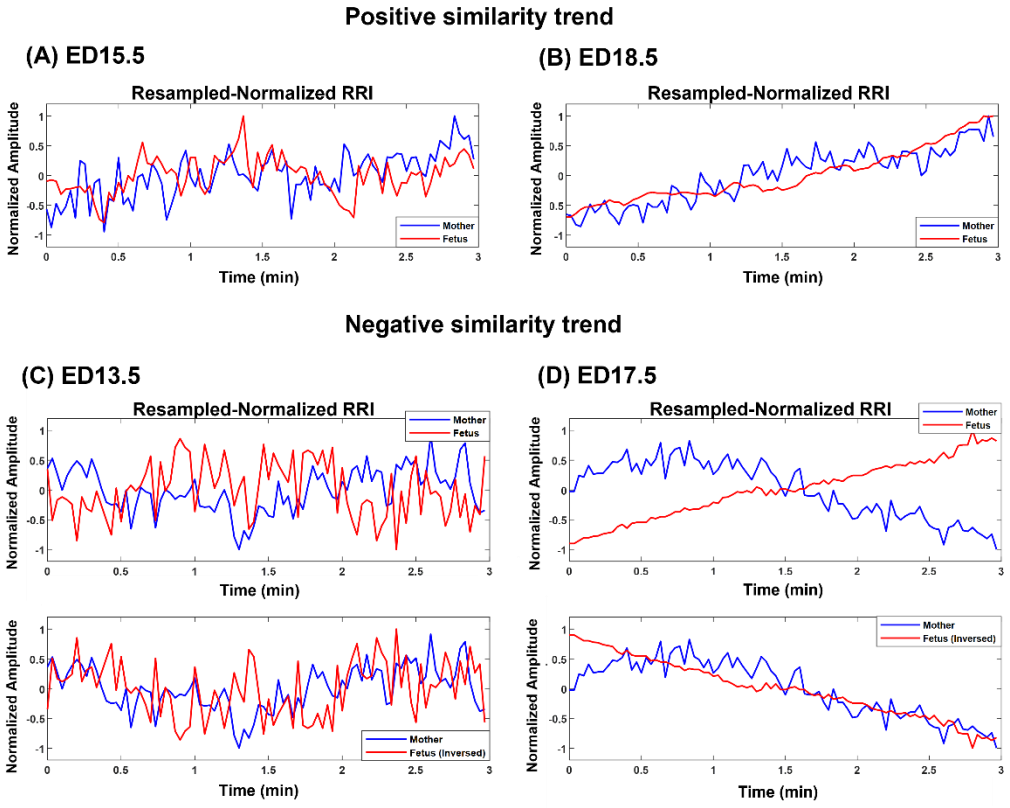

Figure 15: Demonstration of maternal and fetal RR interval (RRI) similarities. All panels show resampled normalized maternal (blue) and fetal (red) RRI. (A) ED15.5, CCm1: 0.42, CCm2: 0.27, coherence low frequency (CLF): 0.084, coherence high frequency (CHF): 0.074. (B) ED18.5, CC1: 0.82, CC2: 0.67, CLF: 0.98, CHF: 0.92. (C) ED13.5, CCm1: 0.29, CCm2: - 0.18, CLF: 0.086, CHF: 0.074. (D) ED17.5, CCm1: 0.85, CCm2: - 0.85, CLF: 0.097, CHF: 0.088.

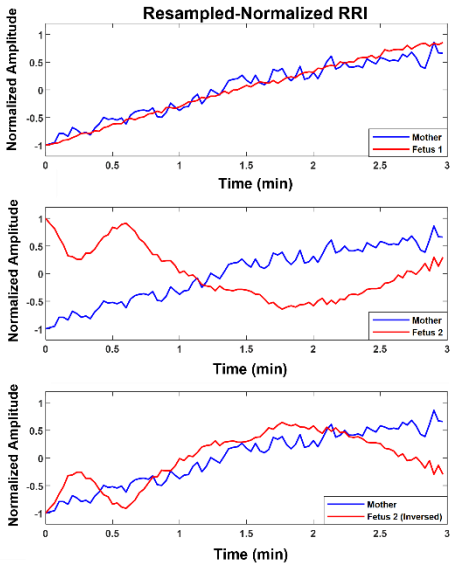

Figure 16: Example of similarity trend of two fetuses from the same mother. The figure shows resampled normalized maternal (blue) and fetal (red) RR interval (RRI) from embryonic day 17.5 (ED17.5). The top panel shows RRI for fetus 1 and the middle and bottom panels show the same for fetus 2. For fetus 1 (top panel), CCm1, CCm2, coherence low frequency (CLF) and coherence high frequency (CHF) values were as follows, 0.92, 0.92, 0.098 and 0.093, respectively. For fetus 2, the same latter values were as follows: 0.83, - 0.60, 0.098 and 0.092, respectively.

- *The degree of similarity between maternal and fetal RRI increases with fetal age*

Figure 17 shows the boxplots of CCm1 (A), CCm2 (B), CLF (C), and CHF (D) coefficients. In each plot, the value of correlation between the coefficient with EDs is shown as *r*. In all plots, there is an increasing trend in the coefficients indicating an increase in similarity with fetal development. Comparison of means analysis shows that there were no significant differences between any of the developmental stages in CCm2 (Figure 17B), on the other hand, some differences were found in the rest of the figures. In Figure 17A, CCm1 values at ED17.5 and ED18.5 were significantly higher than in the previous developmental stages. In Figure 17C, CLF values at ED13.5 were significantly lower than ED15.5, ED17.5, and ED18.5. In Figure 4D, CLF values at E18.5 were significantly higher than ED15.5 and ED13.5, also, CLF values at ED17.5 and ED15.5 were significantly higher than ED13.5. The correlation coefficients show a positive significant correlation and based on the *r*-value of CCm2 coefficient, it is indicated that the probability of finding positive similarity trends increase with fetal growth.

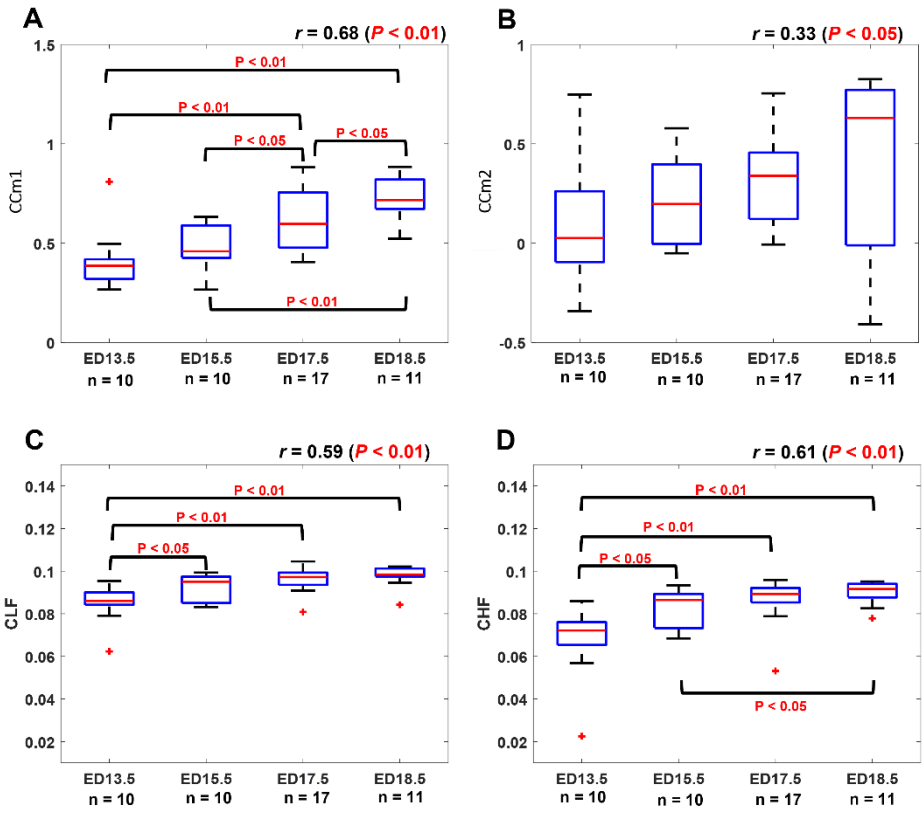

Figure 17: Similarity coefficients at different developmental stages. The similarity between maternal and fetal RR interval (RRI) was quantified by using four coefficients: (A) CC1m(B) CCm2 (C) coherence low frequency (CLF). (D) coherence high frequency (CHF). The value of correlation between the coefficient and embryonic days (EDs) is indicated as *r* above the plot.

6.3.2 ASD mouse model

- Similarity patterns in VPA-treated mice are disturbed

The results in Figure 17 show that similarities are indicators of fetal development. Hence, we conducted a comparison of means analysis between VPA and saline groups in terms of CCm1 (Figure 18A), CCm2 (Figure 18B), CLF (Figure 18C), and CHF (Figure 18D). In all figures, except Figure 18B, it is shown that the saline coefficient values at ED15.5 are significantly higher than that of VPA. With respect to the comparison at ED18.5, all figures show that the saline group coefficients were found to be higher than that of VPA group but the differences were not significant.

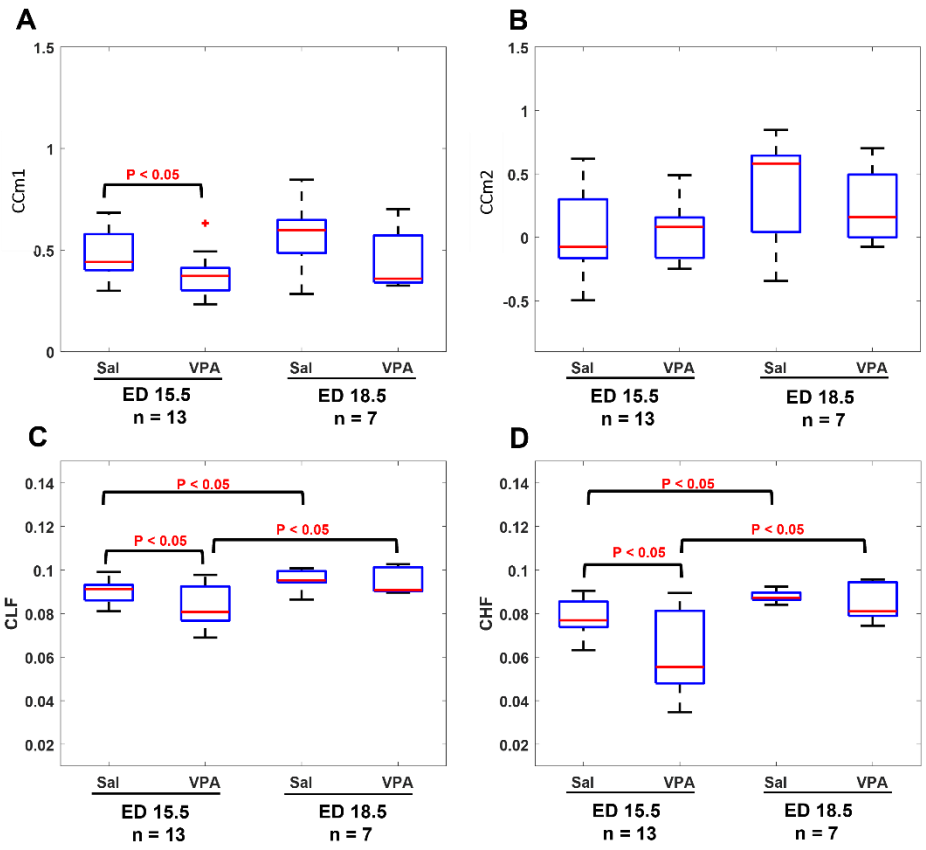

Figure 18: Comparison between saline (sal) group and valproic acid (VPA) groups at embryonic day (ED) 15.5 and ED18.5. (A) CCm1 coefficient. (B) CCm2 coefficient. (C) coherence low frequency (CLF) coefficient. (D) coherence high frequency (CHF) coefficient.

6.4 Discussion and physiological implications

We demonstrated that changes exhibited by maternal and fetal RRI share similarities between them in Figure 15A-D and Figure 16. Similarities were found to follow positive trends (Figure 15A-B) or negative trends (Figure 15C-D). The quantity addressed here as similar is the simultaneous rate of change in maternal and fetal RRI. HRV is controlled by ANS and since both maternal and fetal blood circulatory systems and ANS are separated and work independently, the presence of similarities between both RRI suggests the presence of a mediator between both. The mediator functions as a means of communication between maternal and fetal ANS systems. The CLF and CHF results shown in Figure 15C-D indicate the presence of frequency entrainment between the mother and fetus, which suggests that the entrainment of ANS function could be important as a mediator between the mother and fetus. Figure 16 shows that at a particular time, fetuses belonging to the same mother may interact differently with maternal HR and this implies differences in mediator's influences. Since each fetus has an independent placenta, which is the point of connection between the mother and its child, we expect that the effect of the mediator could

be modified by placental functions and/or factors such as hormones related to the placenta. The exact reason behind the similarity is unknown but, according to Figure 17A-D, it seems that the degree of similarity is associated with fetal development. The more advanced the fetal age is, the more fRRI mimics mRRI.

Figure 17A-B provides CC results in the time domain and Figure 17C-D provides the same in the frequency domain. According to Figure 17A-B, the *r*-value in CCm2 (Figure 17B) was lower than that of CCm1 (Figure 17A), in addition, the comparison of means analysis showed that there were no differences between any of the developmental stages in CCm2. This implies that CCm1 is more indicative of fetal development compared to CCm2. Since CCm1, which was evaluated by absolute value, showed a better association with fetal development than CCm2, development needs to have an increased correlation between mother and fetus, whether positive or negative. Positive and negative correlations between mother and fetus may have some significance, but we cannot elaborate more about them in this study, and we believe that they need to be verified by other approaches. With respect to frequency-based CC analysis, it is revealed that both CLF and CHF were indicative of fetal development.

Previously (85), we used HRV analysis to assess fetal ANS development in which we considered the LF band as an indicator of the sympathetic and parasympathetic systems activity and the HF band as an indicator of the parasympathetic system activity. We do not know how our CLF and CHF associate exactly with either maternal or fetal sympathetic or parasympathetic systems, but we speculate that they associate with ANS activity in general. Mathematically, MSC measures how two signals correlate or are similar in the frequency domain (87), and in our study, the two signals consisted of maternal and fetal RRI, therefore, CLF and CHF are a combined measure of maternal and fetal HF and LF. In our study, the CHF was more efficient compared to CLF in terms of distinguishing between developmental stages. In Figure 17D, there was a significant difference between ED15.5 and ED18.5 whereas the same was absent in Figure 17C. The latter pattern was observed in our earlier study (85) in which we found that the fetal HF band was significantly more correlated to EDs compared to LF.

The results from fetal development highlight this fact, an association between maternal and fetal RRI or ANS is a feature of the development, and disturbances in such correlation is expected to impair fetal development. In ASD mouse model (Figure 18A-D), it is revealed that there were significant differences between control and VPA groups in CCm1, CLF, and CHF values at ED15.5. As in the case of fetal development, CCm1 was found to be more appropriate than CCm2 in this study, because we could not detect any differences due to VPA administration by CCm2. At ED18.5, all four values in VPA group

were found to be generally lower but with no significance. The absence of significance implies that VPA mice could eventually achieve development, but compared to the control group, their development was delayed, and this could be a feature of ASD that is observed only in the fetal period.

The main conclusion that can be highlighted from Figure 18A-D is disturbances in communication between maternal and fetal ANS or HRV is a feature of ASD. It is intriguing that such disturbances were found to be manifested in ED15.5 only which suggests that impairment in fetal neural development could be masked with fetal age and growth and the effect of such impairment seems to take effect after childbirth and growth. The findings in Figure 18A-D imply that the miscommunication that started between maternal and fetal HR in the intrauterine environment gets manifested as miscommunication between the child and his/her surroundings after birth. These results are consistent with the DOHaD and fetal programming theories which associate the origin of adulthood disorders with the prenatal period (4,2,88,89).

Comparison between Figure 17 and Figure 18 show that CCm2 and CHF trends were consistent in both figures. On the other hand, CCm1 and CLF trends were different between both figures in terms of the difference between ED15.5 and ED18.5. In Figure 17A and Figure 18C, the differences were significant whereas they were not significant in Figure 17C and Figure 18A. Although it is not shown in Figure 17C, the *p*-value for the difference between ED15.5 and ED18.5 was 0.053 which is close to the significance level. The absence of significance between ED15.5 and ED18.5 in Figure 18A could be attributed to two reasons. The first is the lower sample size at ED18.5 (ASD mouse model, Figure 18) and the second reason could be attributed to the anesthetic effect. As was demonstrated in the methods section, 2 segments of 3-min were selected randomly from the ECG record for analysis, and such selections were made at the beginning or end of the recordings. Since anesthesia is known to affect HRs in mice (90,91), the effect of anesthesia is expected to change along the recording. For example, the analysis of HR at the beginning of the recordings could be different from the end of the recordings. The effect of anesthesia is a limitation in our study.

There are several limitations to our study. MSC calculation requires signals to have the same lengths, therefore we resampled our signals to unify lengths. As a result of resampling, information regarding CHF was partially lost. CC analysis was used to calculate CC2 to assess directionality in the similarity between maternal and fetal RRI. In Figure 17, the *r* value was low in In Figure 17B, also, there were no significant differences between any of the developmental stages in Figure 17B. In Figure 18, the

CC2 value was not effective in distinguishing between VPA and saline. Hence, we think that more research is needed to effectively estimate the directionality in maternal-fetal RRI similarity.

Here, we analyzed the data retrospectively and the anesthesia mixture (ketamine/xylazine/isoflurane) that was used during ECG recordings is known to affect HR in mice (90,91). In humans, fetal HR and HRV are known to be affected by fetal gender and behavioral states (40,38) and we expect the same effect to exist in mice. Therefore, we speculate that fetal gender, behavioral states, and anesthesia affected CC, CLF, and CHF values in our study. Due to our retrospective design, we did not have further information regarding fetal gender. The lower number of subjects of saline and VPA at ED18.5 was another limitation.

Additional remarks on VPA-Saline differences

In addition to the maternal-fetal RRI similarities in mice, a simple correlation analysis between maternal and fetal average RRI collected over 1-min segments was performed for the ED15.5 data. A total number of 56 1-min segments were collected from 12 saline mice and a total of 54 of the same were collected from 13 VPA mice. The results of correlation analysis revealed that the linear correlation between maternal and fetal RRI was significantly positive in the saline mice group whereas the correlation was significantly negative in the VPA group, Figure 19. The details of this study are found in (92).

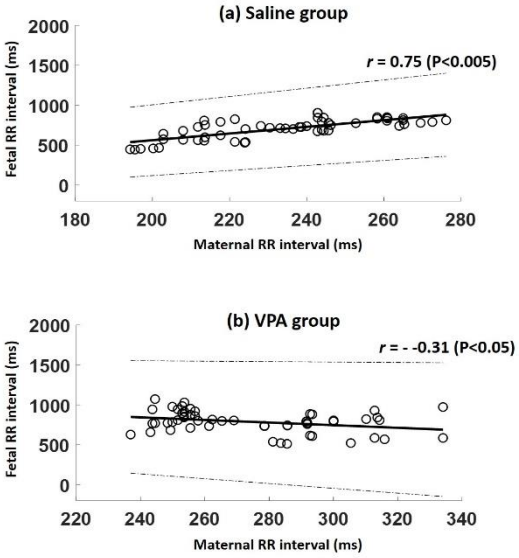

Figure 19: Comparison between saline and VPA in terms of fetal and maternal RRI correlation. (a) Maternal RRI is strongly positively correlated with fetal RRI in saline. (b) Maternal RRI is negatively correlated with fetal RRI in VPA.

The mechanism by which VPA affects fetal development is still unknown, hence, it is unknown how the VPA affects the correlation or similarities between maternal and fetal RRI. VPA is known to cause congenital heart defects such as arterial and ventricular septal defects and improper closure of the septum may mix oxygenated with deoxygenated blood, and this can eventually lead to increased flow to the lung and heart failure (93). Hence, due to the latter, disturbance in the interaction of fetal heart with the maternal heart is expected. Fetal cardiac defects caused by VPA are yet to be understood, however, previous literature addressed that such defects may arise due to inhibition of the histone deacetylase. Histone deacetylase plays a role in gene expression therefore its inhibition may lead to defects in the

formation of the heart (93). VPA is also known to cause neural tube defects and we expect that this could disturb maternal-fetal RRI interaction. Kristin et al. (94). demonstrated that VPA can bind to folate receptors in the epithelial cells of the intestine. The binding of VPA to the folate receptors may lead to folate deficiency in pregnant women which will eventually lead to a reduced transfer of folate through the placenta to the developing fetus (94).

6.5 Use of mouse models to understand physiological processes

In this chapter data from mice were used to examine the presence of similarities between maternal and fetal RRI. In addition, similarity patterns in the autism mouse model were investigated. Similar to humans, the similarity between maternal and fetal RRI in mice had positive and negative patterns. Furthermore, the degree of similarity increased with fetal development. However, the likeliness of the occurrence of negative similarity trends increased with fetal development in humans, on the other hand, the likeliness of the occurrence of positive similarity trends increased with fetal development in mice. This difference between humans and mice could be attributed to the difference in their ANS functionality. For example, in our earlier study (85), we found that maternal and fetal HRV parameters decreased with fetal development in mice. In contrast, here, we found that the same increased with fetal development Table 1.

In addition to the ANS differences, differences related to cardiac functionality could also be related to the difference in the similarity patterns between humans and mice. For example, fRRI values are higher than that of the mother, on the other hand, the opposite is true in humans. Also, in our earlier studies (95,96), we developed models to predict the end of T-waves of ECG in mice (95) and humans (96). The model predicts an end of a T wave based on a function R(t) that was developed based on the discharging phase of a capacitor in an RC circuit. The model was validated with simultaneously recorded Doppler Ultrasound records. Based on the model, we found that, in humans, the end of a T-wave was proportional to RRI in normal subjects but the same was not observed in mice. In mice, the end of a T wave occurred earlier compared to a T end in a human fECG within an RRI, **Figure 20**.

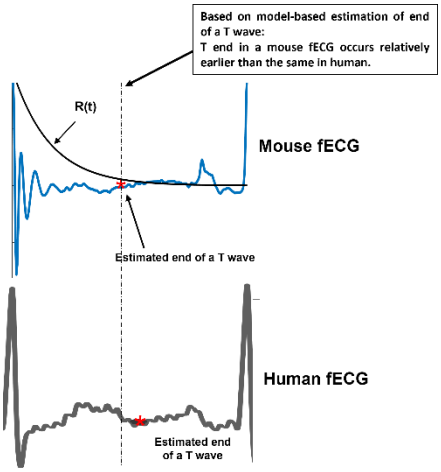

Figure 20: Comparison between human and mouse fetal electrocardiogram (fECG) in terms of model-based estimation of an end of a T wave. This figure shows that a model-based estimation of end of a T wave occurs earlier in a mouse fECG compared to a human fECG.

Despite the differences between mice and humans, studies that entail mice can still be used to get an overall comprehension of the etiology of diseases. Here, we found that disturbances in the similarity between maternal and fetal RRI could be a feature of autism during the prenatal period. Nevertheless, more research with more sample size is needed.

6.6 Conclusion and Limitation

This chapter highlighted the presence of similarities between maternal and fetal RRI tachograms in mice. Similarities were quantified by using four correlation coefficients and it was found that the degree of similarity increased with fetal age in typical fetal mouse development. In this chapter, an investigation of the similarity patterns in ASD mouse model treated with VPA was conducted. A comparison of means analysis between VPA and saline mice showed that the correlation coefficients were generally reduced in VPA mice indicating a disturbance in the rhythm or regulation by which fetal and maternal HRs interact. Hence, it can be concluded that impairment in fetal and maternal HRs interaction could be a possible feature of ASD during the perinatal period.

Chapter 7: Conclusion

7.1 Conclusion and Future Work

In this thesis, the presence of similarity between maternal and fetal RRI tachograms in humans and mice was discussed. The degree of similarity was quantified by CC analysis and MSC analysis (only in mice) and results showed that similarity is associated with fetal development. In both humans and mice, two similarity patterns were identified, negative and positive. In humans, the negative similarity trends seemed to prevail at late fetal age, but the opposite seemed to occur in mice. It is unknown what causes maternal and fetal RRI to associate but it is expected that the cause is linked to the placenta. Our results from human subjects showed that the CC coefficients were linked to mVLF, but more research is needed to verify this as it is expected that different body postures may affect the similarity and ANS activity. Due to different body postures, different associations between maternal and fetal HRV with CC coefficients are expected to be found.

With respect to mice, similarities were associated with typical development, and it was found that disturbances in them were linked to ASD. However, further research is needed to confirm how similarity patterns could change with ASD. The main challenge with analyzing mice data is the effect of anesthesia. For example, in Figure 15B, Figure 15D, and Figure 16, it is shown that maternal and fetal RRI tachograms demonstrate straight increasing lines, and such patterns were not found in human data. It is expected that these straight lines occur due to anesthesia. Within these straight lines, some fluctuations could hold more meanings related to fetal ANS functionality and development. The anesthetic effect is difficult to negate which compromises a great limitation.

Studying the similarity patterns could assist in fetal development assessments. As was discussed in Chapter 4, the presence of similarities suggests the need to develop biomarkers depending on both HRs and this can potentially enhance fetal well-being and pregnancy outcomes. Further, as was addressed in chapter 5, AI-based models may enhance fetal health assessments. It is worth mentioning that developing biomarkers and AI models based on the fact that similarity exists would be meaningful after investigating how similarity patterns change with fetal abnormalities. All of our human data that was discussed here

composed of healthy fetuses, therefore, we could not compare results between healthy and abnormal fetuses. Also, the data was collected from human subjects composed of women with different medical complications. It is expected that such complications affected the results, but due to the limited knowledge in the field, it is unknown to what extent the results were affected.

Here, the similarity was quantified by means of CC and MSC (in mice only) analyses, and more research is needed to confirm the efficiency of such analyses to quantify similarity in relation to fetal development. Also, the effect of window size should be investigated further.

Appendix A

Supplementary Table 1: Detailed information about the participants (n=172)

Maternal Condition	Number of cases	GA (weeks)	Age (years)
Normal	44	20 - 39	22 - 44
Central nervous system (CNS) disease	11	23 - 38	22 - 40
Essential hypertension	3	21 - 37	29 - 42
Blood disease	4	23 - 38	27 - 41
Thyroid disease	1	28	38
Mental Illness	13	22 - 39	27 - 40
Respiratory disease	9	23 - 40	27 - 38
Gestational Diabetes	5	19 - 38	23 - 34
Uterine/appendix disease (UAD)	19	20 - 38	29 - 43
Autoimmune disease	10	25 - 39	29 - 36
Heart disease	3	23 - 26	25 - 33
Placenta previa	6	20 -36	31 - 40
Bone and muscle system disease	2	28 & 32	33
Kidney disease	2	28	32
Pre-eclampsia	1	37	27
Diabetes	1	37	32
Psoriasis vulgaris	1	33	32
Osler's disease	1	36	32
Cervical weakness	1	39	30
Blood disease & gestational diabetes	1	33	41
Cervical weakness & gestational diabetes	1	22	41
Kidney and respiratory diseases	1	37	32
UAD & autoimmune disease	6	26 - 38	28 - 34
UAD & Thyroid disease	2	32 & 39	26 & 37
UAD & digestive system disease	1	20	41
Thyroid and blood diseases	1	23	37
Thyroid and autoimmune disease	1	24	30
Autoimmune disease and placenta previa	1	37	39
Respiratory disease and mental illness	1	20	38
Mental illness and placenta previa	1	37	32
UAD & Mental illness	3	20 - 38	25 - 34
UAD & respiratory disease	2	20 & 39	38 & 45
UAD & Bone and muscle system disease	1	23	44
UAD & Urinary system disease	1	38	39
CNS & Bone and muscle system disease	1	37	42
Gestational diabetes & placenta previa	1	33	30
UAD & gestational diabetes	1	26	34
Respiratory disease & placenta previa	2	35 & 37	35 & 39
UAD & essential hypertension & thyroid disease	1	38	41
UAD & placenta previa	1	33	32
UAD & CNS	1	23	35
Placenta previa & cervical weakness	1	25	35
Heart disease and thyroid disease	1	20	43
Heart disease & respiratory disease and CNS	1	2	27

Appendix B

```
%*********************************************************
%******R Peak detection and RRI calculation codes*****************************%
%*********************************************************

  interv=1:300000; %Specify the duration (For mice it is 180000)
  dataf=fECG(interv); %or mECG
  dataf=dataf./max(dataf); % To normalize the data


%*****R peak detection******* %

data2=dataf;
cld=find(data2<0);
data2(cld)=0;
yf = abs(data2).^2; %Magnify the signal in order to find the R-peaks
my=max(yf);  % Find the maximum value of R-peak
minp=0.11*my;  % Set the minimum peak as x% of the maximum
tm=1:length(yf);

[qrspeaksf,locrf] = findpeaks(yf,tm,'MinPeakHeight',minp,...
    'MinPeakDistance',300);  %Set minimum peak height and minimum interval values

%plotting detected peaks
figure
plot(tm,dataf)
hold on
plot(locrf,sqrt(qrspeaksf),'r*')
xlabel('milliseconds'); ylabel('Amplitude');
title('R Peaks')

%*****RR interval calculation******* %

diff_locrf=diff(locrf); %Find the intervals of RR
```

Appendix C

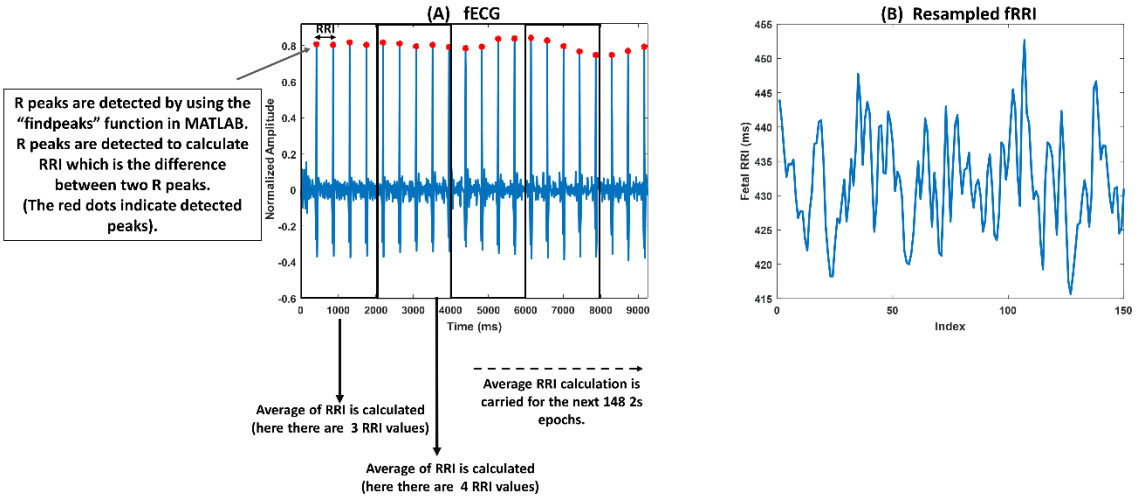

Example of RR interval (RRI) resampling at 0.5Hz (2 seconds). (A) The figure shows the original fetal electrocardiogram (fECG) trace with detected R peaks (red dots). The average RRI was calculated per 2 second epoch. (B) the figure shows the resampled RRI.

Appendix D

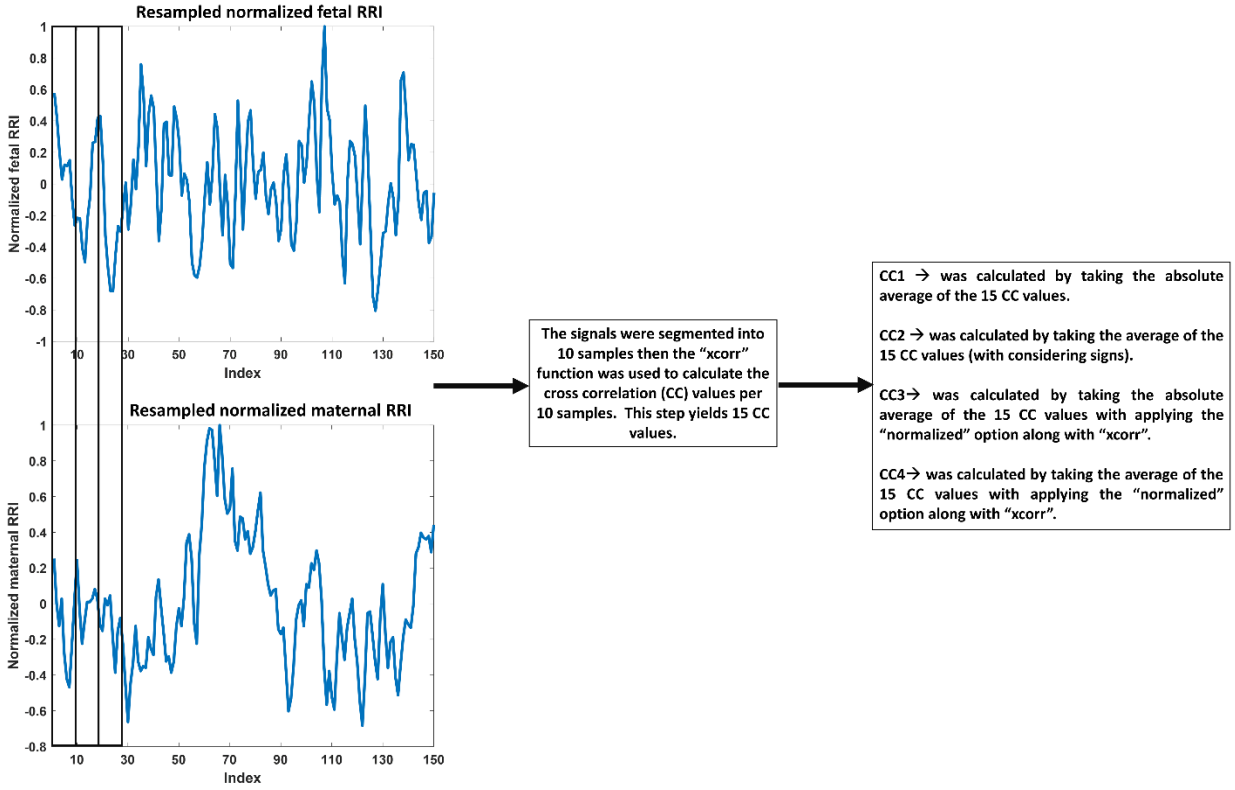

Cross-correlation (CC) calculation. The figure provides an illustrative summary of the steps that were followed to calculate CC1, CC2, CC3 and CC4 from resampled normalized maternal and fetal RR interval (RRI). (The figure of fetal RRI is the same as the one in supplementary figure 2B).

Appendix E

```
%*********************************************************
%******Resampling and Cross-correlation analysis***********%
%*********************************************************


close all;
 clear;clc

fctrs=1;
      fetal_d=xlsread('RR_fixed',1);  %read fetal RR interval and R location
    maternal_d=xlsread('RR_fixed',2); %read maternal RR interval and R location

% %
frr=fetal_d(:,1); mrr=maternal_d(:,1);  %assign fetal and maternal RR interval values
to variables
M_tHR=((maternal_d(:,2))./1000)'; %assign fetal R peak location to a variable
F_tHR=((fetal_d(:,2))./1000)'; %assign maternal R peak location to a variable

sF=single(F_tHR.*1000); sM=single(M_tHR.*1000);

fs=1000; % sampling frequency

%***Humans***** set up resampling parameters ***********
Xt=2000; % resampling freqeuncy 0.5Hz
pts=150; % Number of samples after resampling
mxtx=300000; % original sample size for an ECG signal (5 minutes * fs)

%***MICE**** set up resampling parameters **********
%Xt=2000; % resampling freqeuncy 0.5Hz
%pts=90; % Number of samples after resampling
%mxtx=180000; % original sample size for an ECG signal (5 minutes * fs)


%% ***** Resample maternal RR interval ********%
f1=1;  f2=Xt;
nMrr=[]; nmt=sM; mbts=[];

for i=1:Xt:sM(end)

   tm= find(sM>=f1 & sM<f2); % find R peaks within the specified window size

    %++++++++++++++++++++++++++++++++++++++++++++++++++++++++++
   % set up a condition, in case only one R peak is found within 2000 s
   % window size, the number of R peak will be set up as 1, and the RR
   % interval value will be set up as the difference between the current R
   % peak and the previous one

   if length(tm)>1
```

```
   nMrr= [nMrr;nanmean(diff(sM(tm)))];  % Resampled signal
   mbts=[mbts;length(tm)]; % number of R peaks per 2 seconds
   else

     nMrr= [nMrr;mrr(tm)]; % Resampled signal
     mbts=[mbts;1]; % Number of R peaks per 2 seconds
   end
  %+++++++++++++++++++++++++++++++++++++++++++

    f1=f2;
    f2=f2+Xt;
end

%% ***** Resample fetal RR interval ********%
f1=1;  f2=Xt;
nfrr=[]; nmt=sF;
fbts=[];

for i=1:Xt:sF(end)

   tm= find (sF>=f1 & sF<f2);

   %+++++++++++++++++++++++++++++++++++++++++++++++++++++++++
   % set up a condition, in case only one R peak is found within 2000 s
   % window size, the number of R peak will be set up as 1, and the RR
   % interval value will be set up as the difference between the current R
   % peak and the previous one

   if length(tm)>1

   nfrr= [nfrr;mean(diff(sF(tm)))]; %resampled RR interval
   fbts=[fbts;length(tm)];  %Number of R peaks per 2 minutes

   else

   nfrr= [nfrr;frr(tm)]; %resampled RR interval
   fbts=[fbts;1]; %Number of R peaks per 2 minutes
   end
      %+++++++++++++++++++++++++++++++++++++++++++++++++++++++++

    f1=f2;
    f2=f2+Xt;

end

nMrro=nMrr; nfrro=nfrr; % set the resampled signals into new variables

%Normalize Resampled maternal RR interval
nMrr=nMrr-mean(nMrr);
nMrr=nMrr./max(abs(nMrr));

%Normalize Resampled fetal RR interval
nfrr=nfrr-mean(nfrr);
nfrr=nfrr./max(abs(nfrr));
```

```
%+++++++++++++++++++++++++++++++++++++++++++++++++++++++

%******Human********%
This condition was set up to accomodate for the signals that are 149 in lengths
 tx=1:Xt:mxtx;tx=tx./60000;
 if length(nMrr)<pts & length(nfrr)==pts
    nfrr(end)=[]; tx(end)=[]; fbts(end)=[]; nfrro(end)=[];
 end

%******Mice********%
%This condition was set up to accomodate for the signals that are 99 in lengths
if length(nfrr)<pts & length(nMrr)==pts
      nMrr(end)=[]; tx(end)=[]; mbts(end)=[]; nMrro(end)=[];
 end
 %+++++++++++++++++++++++++++++++++++++++++++++++++++++++



%% *****Cross Correlation analysis******%%

fp=1; ep=10; % 10 samples
Corrm=[]; Corrm2=[];

for i=1:10:pts

    cm=nMrr(fp:ep); %set the maternal 10 samples segment
    cf=nfrr(fp:ep); %set the fetal 10 samples segment

  %Cross correlation calculation (non-normalized)
    [c,lags] = xcorr(cm,cf); Ls=find(lags==0);
    Corrm=[Corrm;c(Ls)];

%Cross correlation calculation (normalized)
[c2,lags2] = xcorr(cm,cf,'normalized'); Ls2=find(lags2==0);
Corrm2=[Corrm2;c2(Ls2)];


  %next 10 samples
    fp=ep+1; ep=10+ep;

    %Terminate the loop at 149 in case the RR inerval signal's maximum
    %length was 149
    if ep==pts &length(nMrr)==pts-1
        ep=pts-1;
    end

end

%CC1 and CC2
[mean (abs(Corrm)) mean (Corrm)]
%CC3 and CC4
[mean (abs(Corrm2)) mean (Corrm2)]
```

```
%% ***Mice ****Magnitude squared coherence analysis*************

[y,x]=mscohere(nfrro,nMrro,10,[],[],pts/(3*60));

% Band division

Finx_LF=find(x<=0.15&x>0.04); % Low frequency
Finx_HF=find(x<=0.25&x>0.15); % High frequency

% CLF
xLF=trapz(x(Finx_LF),y(Finx_LF));
% CHF
xHF=trapz(x(Finx_HF),y(Finx_HF));

% Plotting
figure
area(x,y,'FaceColor',[.6 .6 .6]); xlabel('Frequency (Hz)'); ylabel('(PSD (ms^2/Hz))')
hold on;

area(x(Finx_LF),(y(Finx_LF)),'FaceColor','b');
area(x(Finx_HF),(y(Finx_HF)),'FaceColor','r');
%legend('','LF','HF')
ax = gca;
ax.FontSize = 10; ax.FontWeight = 'bold';
```

Appendix F

Supplementary Table 2: Comparison between group 1 and group 2 in terms of HRV and CC association with GA, n=158

	Group 1 (Low CC3)			Group 2 (High CC3)		
Feature	**Correlation between CC coefficients and GA**					
	median (min – max)	(mean ± SD)	*r*	median (min – max)	(mean ± SD)	*r*
CC1	0.47 (0.11 – 1.3)	0.52 ± 0.24	0.40†	0.58 (0.15 – 2.8)	0.67 ± 0.37	0.40†
CC2	- 0.032 (- 0.10 – 0.81)	- 0.064 ± 0.24	- 0.21†	-0.086 (-1.8 – 1.2)	- 0.12 ± 0.40	- 0.16*
CC3	0.38 (0.21 – 0.65)	0.38 ± 0.08	0.13	0.48 (0.27 – 0.71)	0.48 ± 0.08	0.16
CC4	- 0.016 (- 0.39 – 0.41)	- 0.017 ± 0.14	- 0.23†	-0.030 (- 0.52 – 0.49)	-0.05 ± 0.18	- 0.11
Feature	**Correlation between HRV and GA**					
	Maternal Features		**Fetal features**		**Maternal Features**		**Fetal features**	
	(mean ± SD) median (min – max)	*r*	(mean ± SD) median (min – max)	*r*	(mean ± SD) median (min – max)	*r*	(mean ± SD) median (min – max)	*r*
RRI (ms)	763 ± 117 751 (537 – 1125)	- 0.06	414 ± 25 411 (358 – 512)	0.42†	762 ± 113 757 (530 – 1107)	- 0.01	411 ± 25 407 (351 – 510)	0.37†
SDNN (ms)	32 ± 13 30 (10 – 76)	0.20*	15 ± 6.8 14 (4.0 – 45)	0.37†	37 ± 17 33 (13 – 120)	0.33†	16 ± 7.2 15 (4.5 – 36)	0.57†
SDHR (bpm)	3.4 ± 1.4 3.2 (1.3 – 11)	0.31†	5.3 ± 2.4 5.0 (1.2 – 14)	0.32†	3.8 ± 1.5 3.6 (1.3 – 9.4)	0.39†	5.9 ± 2.6 5.3 (1.7 – 14)	0.52†
VLF (Ln)	6.0 ± 0.78 6.0 (3.9 – 8.0)	0.34†	4.3 ± 1.2 4.3 (0.86 – 7.2)	0.29†	6.3 ± 0.81 6.3 (4.1 – 8.6)	0.37†	4.6 ± 1.1 4.6 (1.8 – 6.8)	0.53†
LF (Ln)	5.1 ± 0.84 5.0 (2.6 – 7.5)	0.08	4.3 ± 0.87 4.3 (1.4 – 6.3)	0.35†	5.1 ± 0.77 5.1 (3.3 – 7.8)	0.19*	4.3 ± 0.81 4.4 (1.6 – 6.5)	0.52†
HF (Ln)	4.8 ± 1.3 4.7 (0 – 7.8)	0.04	2.3 ± 0.79 2.4 (-0.46 – 4.1)	0.49†	4.8 ± 1.2 4.7 (1.1 – 8.0)	0.11	2.2 ± 0.79 2.2 (0.46 – 4.2)	0.53†

*** P < 0.05, † P <0.005, HRV: heart rate (HR) variability, GA: gestational age, CC: cross-correlation, RRI: RR interval, SD: standard deviation, SDNN: SD of normal RRI, SDHR: SD of HR, bpm: beats per minute, VLF: very low frequency power, LF: low frequency power, HF: high frequency power, *r*: spearman correlation coefficient. (The table was made based on CC3BC data set**

References

1. Hall M, George E, Grangerb J. The heart during pregnancy. Rev Esp Cardiol. 2013; 64(11): p. 1045–1050.

2. Barker D. Fetal origins of coronary heart disease. BMJ. 1995; 311: p. 171-174.

3. Institute of Medicine (US) Committee on Improving Birth Outcomes. The problem of low birth weight. In Improving birth outcomes: meeting the challenge in the developing world. Washington (DC): National Academy of Sciences; 2003.

4. Arima Y, Fukuoka H. Developmental origins of health and disease theory in cardiology. J Cardiol. 2020; 76(1): p. 14-17.

5. Fetal blood sampling. [Online]. [cited 2022 July 12. Available from: https://www.stanfordchildrens.org/en/topic/default?id=fetal-blood-sampling-90-P02447.

6. DiPietro J, Raghunathan R, Wu HT, et al. Fetal heart rate during maternal sleep. Dev Psychobiol. 2021; 63(5): p. 945-959.

7. Laar J, Warmerdam G, Verdurmen K, et al. Fetal heart rate variability during pregnancy, obtained from non-invasive electrocardiogram recordings. Acta Obstet Gynecol Scand. 2014; 93(1): p. 93-101.

8. Amorim-Costa C, Gaio A, Ayres-de-Campos D, et al. Longitudinal changes of cardiotocographic parameters throughout pregnancy: a prospective cohort study comparing small-for-gestational-age and normal fetuses from 24 to 40 weeks.. J Perinat Med. 2017 May; 45(4).

9. Odendaal H, Kieser E, Nel D, et al. Effects of low maternal heart rate on fetal growth and birthweight. Int J Gynaecol Obstet. 2020; 146(2): p. 250-256.

10. Yang C, Chao TC, Kuo T, et al. Preeclamptic pregnancy is associated with increased sympathetic and decreased parasympathetic control of HR. Am J Physiol Heart Circ Physiol. 2000; 278(4): p. 1269-1273.

11. Vries J, Visser E, Mulder J, et al. Diurnal and other variations in fetal movement and heart rate patterns at 20-22 weeks. Early Hum Dev. 1987; 15(6): p. 333-348.

12. Lunshof S, Boer K, Hoffen H, et al. Fetal and maternal diurnal rhythms during the third trimester of normal pregnancy: outcomes of computerized analysis of continuous twenty-four-hour fetal heart rate recordings. Am J Obstet Gynecol. 1998; 178(2): p. 247-254.

13. Monk C, Fifer W, Myers M, et al. Maternal stress responses and anxiety during pregnancy: effects on fetal heart rate. Dev Psychobiol. 2000; 36(1): p. 67-77.

14. Leeuwen PV, Geue D, Thiel M, et al. Influence of paced maternal breathing on fetal–maternal heart rate coordination. PNAS. 2009; 106(33): p. 13662-13666.

15. Husin H, Schleger F, Bauer I, et al. Maternal weight, weight gain, and metabolism are associated with changes in fetal heart rate and variability. Obesity. 2020; 28(1): p. 114 - 121.

16. Fetal monitoring. [Online]. [cited 2022 June 13. Available from: https://www.pregnancybirthbaby.org.au/fetal-monitoring.

17. Bekedam D, Mulder E, Snijders R, et al. The effects of maternal hyperoxia on fetal breathing movements, body movements and heart rate variation in growth retarded fetuses. Early Hum Dev. 1991 Dec; 27(3).

18. Patrick J, Campbell K, Carmichael L, et al. Influence of maternal heart rate and gross fetal body movements on the daily pattern of fetal heart rate near term. Am J Obstet Gynecol. 1982; 144(5): p. 533-558.

19. Leeuwen P, Geue D, Lange S, et al. Is there evidence of fetal-maternal heart rate synchronization? BMC Physiol. 2003; 3(2).

20. Dipietro J, Irizarry R, Costigan K, et al. The psychophysiology of the maternal-fetal relationship. Psychophysiology. 2004; 41(4): p. 510-520.

21. Sletten J, Kiserud T, Kessler J. Effect of uterine contractions on fetal heart rate in pregnancy: a prospective observational study. Acta Obstet Gynecol Scand. 2016; 95(10): p. 1129-1135.

22. Marzbanrad F, Kimura Y, Palaniswami M, et al. Quantifying the Interactions between Maternal and Fetal Heart Rates by Transfer Entropy. PLoS One. 2015; 10(12).

23. Khandoker A, Yoshida C, Kasahara Y, et al. Regulation of Maternal-Fetal Heart Rates and Coupling in Mice Fetuses. In 2018 40th Annual International Conference of the IEEE Engineering in Medicine and Biology Society (EMBC); 2018; Honolulu, HI, USA.

24. Leeuwen P, Gustafson K, Cysarz D, et al. Aerobic exercise during pregnancy and presence of fetal-maternal heart rate synchronization. PLoS One. 2014; 9(8).

25. Lakhno I. Autonomic imbalance captures maternal and fetal circulatory response to pre-eclampsia. Clin Hypertens.. 2017; 23(5).

26. Lakhno I. The relationship between fetal and maternal hemodynamic oscillations in normal and growth restricted fetuses. Athens Journal of Health. 2017; 4(1): p. 51-60.

27. Khandoker A, Ibrahim E, Oshio S, et al. Validation of Beat by Beat Fetal Heart Signals Acquired from Four-Channel Fetal Phonocardiogram with Fetal Electrocardiogram in Healthy Late Pregnancy. Sci Rep. 2018; 8.

28. Sato M, Kimura Y, Chida S, et al. A novel extraction method of fetal flectrocardiogram from the composite abdominal signal. IEEE Trans Biomed Eng. 2007; 54(1): p. 49-58.

29. R Wave Detection in the ECG. [Online]. [cited 2022 Aug 21. Available from: https://www.mathworks.com/help/wavelet/ug/r-wave-detection-in-the-ecg.html.

30. Task Force of the European Society of Cardiology the North American Society of Pacing Electrophysiology. Heart rate variability: standards of measurement, physiological interpretation, and clinical Use. Circulation. 1996; 93(5): p. 1043-1065.

31. Thu T, Hernández A, Costet N, et al. Improving methodology in heart rate variability analysis for the premature infants: Impact of the time length - PubMed. PLoS One. 2019; 14(8).

32. Chatow U, Davidson S, Reichman L, et al. Development and maturation of the autonomic nervous system in premature and full-term infants using spectral analysis of heart rate fluctuations. Pediatr Res. 1995; 37(3): p. 294-302.

33. xcorr. [Online]. [cited 2022 October 10. Available from: https://www.mathworks.com/help/matlab/ref/xcorr.html.

34. Imperial College London. Correlation. [Online]. [cited 2022 Dec 20. Available from: http://www.ee.ic.ac.uk/hp/staff/dmb/courses/E1Fourier/00800_Correlation.pdf.

35. BenSaïda A. Shapiro-Wilk and Shapiro-Francia normality tests. [Online].; 2014 [cited 2022 April 19. Available from: https://www.mathworks.com/matlabcentral/fileexchange/13964-shapiro-wilk-and-shapiro-francia-normality-tests.

36. Shaffer F, Ginsberg J. An overview of heart rate variability metrics and norms. Front Public Health.. 2017; 5(258).

37. Díaz P, Powell T, Jansson T. The role of placental nutrient sensing in maternal-fetal resource allocation. Biol Reprod. 2014; 91(4).

38. Nijhuis J, Prechtl H, Martin J, et al. Are there behavioural states in the human fetus? Early Hum Dev. 1982; 6(2): p. 177-195.

39. Pillai M, James D. The development of fetal heart rate patterns during normal pregnancy. Obstet Gynecol. 1990 Nov; 76(5).

40. DiPietro J, Costigan K, Voegtline K. Studies in Fetal Behavior: Revisited, Renewed, and Reimagined. Monogr Soc Res Child Dev.. 2015; 80(3): p. vii–vii94.

41. May L, Knowlton J, Hanson J, et al. Effects of exercise during pregnancy on maternal heart rate and heart rate variability. PM R. 2016; 8(7): p. 611-617.

42. Mizuno T, Tamakoshi K, Tanabe K. Anxiety during pregnancy and autonomic nervous system activity: A longitudinal observational and cross-sectional study. J Psychosom Res. 2017; 99: p. 105-111.

43. Walther T, Wessel N, Baumert M, et al. Longitudinal analysis of heart rate variability in chronic hypertensive pregnancy. Hypertens Res. 2005; 28(2): p. 113-118.

44. Shaffer F, McCraty R, Zerr C. A healthy heart is not a metronome: an integrative review of the heart's anatomy and heart rate variability. Front Psychol.. 2014; 5.

45. Taylor J, Carr D, Myers C, et al. Mechanisms underlying very-low-frequency RR-interval oscillations in humans. Circulation. 1998; 98(6): p. 547-555.

46. Akselrod S, Gordon D, Ubel F, et al. Power spectrum analysis of heart rate fluctuation: a quantitative probe of beat-to-beat cardiovascular control. Science. 1981; 213(4504): p. 220-222.

47. Nkurikiyeyezu K, Suzuki Y, Lopez G. Heart rate variability as a predictive biomarker of thermal comfort. JAIHC. 2017; 9: p. 1465–1477.

48. Fleisher L, Frank M, Sessler D, et al. Thermoregulation and heart rate variability. Clin Sci (Lond). 1996; 90(2): p. 97-103.

49. Myatt L. Control of vascular resistance in the human placenta. Placenta. 1992; 13(4): p. 329-341.

50. Robinsona D, Kleina S. Pregnancy and pregnancy-associated hormones alter immune responses and disease pathogenesis. Horm Behav. 2013; 62(3): p. 263–271.

51. Ojeda N, Grigore D, Robertson E, et al. Estrogen protects against increased blood pressure in postpubertal female growth restricted offspring. Hypertension. 2007; 50(4).

52. Gallagher P, Li P, Lenhart J, et al. Estrogen regulation of angiotensin-converting enzyme mRNA. Hypertension. 1999; 33(1).

53. Brosnihan KB, Hodgin J, Smithies O, et al. Tissue-specific regulation of ACE/ACE2 and AT1/AT2 receptor gene expression by oestrogen in apolipoprotein E/oestrogen receptor-alpha knock-out mice. Exp Physiol. 2008; 93(5): p. 658-664.

54. Dhaundiyal A, Kumari P, Sainath S, et al. Is highly expressed ACE 2 in pregnant women “a curse” in times of COVID-19 pandemic? Life Sci.. 2021; 264.

55. Valenti O, Prima F, Renda E, et al. Fetal cardiac function during the first trimester of pregnancy. J Prenat Med.. 2011; 5(3): p. 59-62.

56. Loerup L, Pullon R, Birks J, et al. Trends of blood pressure and heart rate in normal pregnancies: a systematic review and meta-analysis. BMC Med. 2019; 17(1).

57. Watanabe N, Reece J, Polus B. Effects of body position on autonomic regulation of cardiovascular function in young, healthy adults. Chiropr Osteopat.. 2007; 15(19).

58. Li FK, Sheng CS, Zhang DY, et al. Resting heart rate in the supine and sitting positions as predictors of mortality in an elderly Chinese population. J Hypertens. 2019; 37(10): p. 2024-2031.

59. Bernardes J, Gonçalves H, Ayres-de-Campos D, et al. Linear and complex heart rate dynamics vary with sex in relation to fetal behavioural states. Early Hum. Dev. 2008 July; 84(7).

60. Gonçalves H, Fernandes D, Pinto P, et al. Simultaneous monitoring of maternal and fetal heart rate variability during labor in relation with fetal gender. Dev Psychobiol. 2017 Nov; 59(7).

61. Yadav L, Yadav P, Yadav L, et al. Association between obesity and heart rate variability indices: an intuition toward cardiac autonomic alteration – a risk of CVD. Diabetes Metab Syndr Obes. 2017; 10: p. 57-64.

62. Rossi R, Vanderlei L, Gonçalves A, et al. Impact of obesity on autonomic modulation, heart rate and blood pressure in obese young people. Auton Neurosci. 2015; 193: p. 138-141.

63. Tsuji H, Larson M, Venditti F, et al. Impact of reduced heart rate variability on risk for cardiac events. The framingham heart study. Circulation. 1996; 94(11).

64. Sessa F, Anna V, Messina G, et al. Heart rate variability as predictive factor for sudden cardiac death. Aging (Albany NY). 2018 Feb.; 10(2).

65. Hadase M, Azuma , Akihiro , et al. Very low frequency power of heart rate variability is a powerful predictor of clinical prognosis in patients with congestive heart failure. Circ J. 2004 Apr.; 2004(68).

66. Deo R. Machine learning in medicine. Circulation.. 2018 Nov; 132(20).

67. Hsich E, Gorodeski E, Blackstone E, et al. Identifying important risk factors for survival in patient with systolic heart failure using random survival forests. Circ Cardiovasc Qual Outcomes. 2011 Jan; 4(1).

68. Alkhodari M, Jelinek H, Karlas A, et al. Deep learning predicts heart failure with preserved, mid-range, and reduced left ventricular ejection fraction from patient clinical profiles. Front Cardiovasc Med. 2021 Nov; 22.

69. Giraud R, Siegenthaler N, Morel D, et al. Respiratory change in ECG-wave amplitude is a reliable parameter to estimate intravascular volume status. J Clin Monit Comput. 2013 Apr; 27(2).

70. Lorne E, Mahjoub Y, Guinot PG, et al. Respiratory variations of R-wave amplitude in lead II are correlated with stroke volume variations evaluated by transesophageal doppler echocardiography. J Cardiothorac Vasc Anesth. 2012 Jun; 26(3).

71. Almeida-Santos M, Barreto-Filho A, Oliveira J, et al. Aging, heart rate variability and patterns of autonomic regulation of the heart. Arch Gerontol Geriatr. 2016 Mar-Apr; 63(1-8).

72. Young H, Benton D. Heart-rate variability: a biomarker to study the influence of nutrition on physiological and psychological health? Behav Pharmacol.. 2018 Apr; 29.

73. Estévez-Báez M, Machado C, Montes-Brown J, et al. Very high frequency oscillations of heart rate variability in healthy humans and in patients with cardiovascular autonomic neuropathy. Adv Exp Med Biol. 2018; 1070: p. 49-70.

74. Awad M, Khanna R. Support Vector Regression. In Efficient Learning Machines. Berkeley, CA: Apress; 2015. p. 67-80.

75. Understanding Support Vector Machine Regression. [Online]. [cited 2022 June 21. Available from: https://www.mathworks.com/help/stats/understanding-support-vector-machine-regression.

76. Couronné R, Probst P, Boulesteix AL. Random forest versus logistic regression: a large-scale benchmark experiment. BMC Bioinformatics.. 2018 Jul.; 19(270).

77. Lundberg S, Erion G, Chen H, et al. From local explanations to global understanding with explainable AI for trees. Nat Mach Intell. 2020; 2(1).

78. Lundberg S, Lee SI. A unified approach to interpreting model predictions. Advances in Neural Information Processing Systems 30 (NIPS 2017). 2017.

79. Bland J, Altman D. Applying the Right Statistics: Analyses of Measurement Studies. Ultrasound Obstet Gynecol. 2003; 22(1): p. 85-93.

80. Bland J, Altman D. Measuring Agreement in Method Comparison Studies. Stat Methods Med Res. 1999; 8(2): p. 135-160.

81. Mehari Ma, Maeruf H, Robles C, et al. Advanced maternal age pregnancy and its adverse obstetrical and perinatal outcomes in Ayder comprehensive specialized hospital, Northern Ethiopia, 2017: a comparative cross-sectional study. BMC Pregnancy Childbirth. 2020 Jan; 30(1).

82. Montori M, Martínez A, Álvarez C, et al. Advanced maternal age and adverse pregnancy outcomes: A cohort study. Taiwan J Obstet Gynecol. 2021 Jan; 60(1).

83. Rodgers J, Jones J, Bolleddu S, et al. Cardiovascular risks associated with gender and aging. J Cardiovasc Dev Dis.. 2019 Jun; 6(2).

84. Kasahara Y, Yoshida C, Nakanishi K, et al. Alterations in the autonomic nerve activities of prenatal autism model mice treated with valproic acid at different developmental stages. Sci Rep. 2020 October; 10(1).

85. Kasahara Y, Yoshida C, Saito M, et al. Assessments of heart rate and sympathetic and parasympathetic nervous activities of normal mouse fetuses at different stages of fetal development using fetal electrocardiography. Front Physiol. 2021; 8(12).

86. Minato T, Ito T, Kasahara Y, et al. Relationship Between Short Term Variability (STV) and Onset of Cerebral Hemorrhage at Ischemia–Reperfusion Load in Fetal Growth Restricted (FGR) Mice. Front Physiol.. 2018; 9(478).

87. Malekpour S, Gubner J, Setharesc W. Measures of generalized magnitude-squared coherence: differences and similarities. J Franklin Inst. 2018 Mar; 355(5).

88. Kwon E, Kim Y. What is fetal programming?: a lifetime health is under the control of in utero health. Obstet Gynecol Sci.. 2017; 60(6): p. 506-519.

89. Godfrey K, Barker D. Fetal programming and adult health. Public Health Nutr. 2001; 4(2B): p. 611-624.

90. Jr SP, Bačová I, Svorc P, et al. Autonomic nervous system under ketamine/ xylazine and pentobarbital anaesthesia in a Wistar rat model: a chronobiological view. Prague Med Rep. ; 114(2).

91. Tan T, Gao XM, Krawczyszyn M, et al. Assessment of cardiac function by echocardiography in conscious and anesthetized mice: importance of the autonomic nervous system and disease state. J Cardiovasc Pharmacol. 2003 Aug; 42(2).

92. Widatalla N, Khandoker A, Yoshida C, et al. Effect of valproic acid on maternal - fetal heart rates and coupling in mice on embryonic day 15.5 (E15.5). In EMBC 2021; 2021; Mexico.

93. Philbrook N, Nikolovska A, Maciver R, et al. Characterizing the effects of in utero exposure to valproic acid on murine fetal heart development. Birth Defects Res. 2019; 111(19): p. 1551-1560.

94. Fathe K, Palacios A, Finnell R. Novel Mechanism for Valproate-Induced Teratogenicity. Birth Defects Res A Clin Mol Teratol.. 2015; 100(8): p. 592–597.

95. Widatalla N, Funamoto K, Kawataki M, et al. Model-based estimation of QT intervals of mouse fetal electrocardiogram. Biomed. Eng. Online. 2022; 21(45).

96. Widatalla N, Kasahara Y, Kimura Y, et al. Model Based Estimation of QT Intervals in Non-Invasive Fetal ECG Signals. PLOS ONE. 2020; 15(5).